INEEL/EXT-2000-00651
Revision 0

September 2000

Evaluation of OU 7-10 Stage I Soil Moisture Readings

Operable Unit 7-10 (OU 7-10) Staged Interim Action Project Stage I

G. A. Beitel
P. Kuan
C. W. Bishop
N. E. Josten

Idaho Completion Project

Bechtel BWXT Idaho, LLC

21-0111169 LMIT

INEEL/EXT-2000-00651
Revision 0

Evaluation of OU 7-10 Stage I Soil Moisture Readings

Operable Unit 7-10 (OU 7-10)
Staged Interim Action Project Stage I

G. A. Beitel
P. Kuan
C. W. Bishop
N. E. Josten

Published September 2000

Idaho National Engineering and Environmental Laboratory
Idaho Falls, Idaho 83415

Prepared for the
U.S. Department of Energy

Under DOE Idaho Operations Office
Contract DE-AC07-99ID13727

Evaluation of OU 7-10 Stage I Soil Moisture Readings

Operable Unit 7-10 (OU 7-10)
Staged Interim Action Project Stage I

INEEL/EXT-2000-00651

Revision 0

September 2000

James C. Olson 4 October 2000
WAG 7-10 Project Manager

George A. Bethel 9/27/00
Author, OU 7-10 Stage I Systems Engineer

[signature] 9/28/00
Author, Nuclear Analysis

Carolyn W Burley 9/27/00
Author, Integrated Earth Sciences

M. E. Jorgensen 9/26/00
Author, GeoSciences

This page intentionally left blank.

ABSTRACT

Twenty probe-holes were driven into Pit 9 by the OU 7-10 Staged Interim Action Project during November and December 1999. Active and passive neutron and gamma measurements were made during January and February 2000 using neutron gamma logging tools. The results of this logging were provided to the Project by Waste Management Technical Services (WMTS) of Richland, WA in April 2000. The apparent low soil moisture content in the waste zone triggered an evaluation of the significance of those readings. This report presents that evaluation along with the results of the findings and recommendations for future work.

This page intentionally left blank.

Table of Contents

This page intentionally left blank

Evaluation of Stage I Soil Moisture Readings

1. INTRODUCTION

This report was prepared for the OU 7-10 Staged Interim Action Project, Stage I, Phase I, based on the evaluation of data collected during the neutron and gamma logging of 20 probe holes placed in Pit 9. The neutron-neutron data collected and presented by Waste Management Technical Services (WMTS),[25] of Richland, WA, indicated low volumetric moisture content (less than 5 vol%) at a depth correlating with zones in which radiological contamination and/or chlorine were observed. WMTS reported that the apparent volumetric moisture content (in the waste zone) had a minimum value of less than 7.4 vol% (5 wt%) in nineteen of the 20 probe holes. The WMTS report notes that the neutron-neutron "moisture" results correlate reasonably well with the hydrogen concentration based on an independent neutron-capture gamma response in the underburden and overburden. However, there is a dichotomy between these two sensor methods in the waste zone; WMTS suggested that matrix dependent corrections (without being specific) to either or both measurements be identified and applied.

The data interpretation provided by WMTS[25] was based on calibration models representing uniform soils. That interpretation did not account for masking effects caused by the complex composition of the Pit 9 wastes. This document describes models developed to evaluate the interaction of neutrons with materials and configurations known to be in Pit 9. These models included soil and waste matrices. Soil data and moisture behavior in soils at the Subsurface Disposal Area (SDA) and the Cold Test Pit were also reviewed and used along with the neutron-gamma models to interpret this data.

1.1 Objective of the Evaluation

The purpose of the evaluation is to determine if interactions between known waste components and the corresponding measurement tools can explain the extremely low measured moisture content. The apparent disagreement between volumetric moisture content based on neutron measurements and measurements of the 2223 keV hydrogen gamma are also investigated. This information is then used to identify individual waste forms in the Stage I area of Pit 9.

1.2 Summary

Active and passive neutron and spectral gamma measurements using standard nuclear logging measurements were made in Pit 9 in December 1999 and January 2000. The results were provided in a draft report by the subcontractor WMTS of Richland, WA. The observations on moisture content were analyzed with respect to expected waste forms, co-located chlorine concentrations, and expected neutron interactions. The results of that analysis are provided in this report. Key findings are:

- The soil moisture data in the overburden and underburden are consistent with previous SDA soil moisture measurements, and show 20 - 24 vol% moisture.
- The generally observed decrease in apparent moisture (based on thermal neutron measurements) in the waste zone is due to a combination of:
  - a) intact waste packages that preclude the entry of moisture into the package
  - b) voids in the waste
  - c) absorption of neutrons by chlorine.

- Accurate measurements of moisture in the waste zone cannot be made because of a combination of neutrons absorption by chlorine; the existence of voids in the waste; and graphite, combustible, and Series 743 sludge wastes. Two waste forms—combustible and Series 743 sludge—contain hydrogen from paper, plastic, and oils at concentrations that dominate the hydrogen from the maximum water content expected in the wastes or in the soil. Two percent of the drums contain graphite, which is a good moderator without the neutron absorption capacity of soil or other wastes. Therefore, the graphite wastes can provide a high thermal neutron contribution, relative to that expected from soil moisture, independent of water presence.

- Chlorine is the major influence that precludes accurate hydrogen measurements. The concentrations of chlorine in the pit exceeded the calibration range of the nuclear logging tools. It is recommended that the tools be calibrated at higher chlorine levels before additional measurements are made.

2. BACKGROUND

This section provides a brief summary of volumetric moisture data presented in the April 2000 WMTS Report.

2.1 WMTS Report

A draft copy of the OU 7-10 Staged Interim Action Project, Stage I, Phase I logging report[25], was provided April 17, 2000. The report contains data collected from the first 20 probe holes placed in Pit 9. The data had been collected in neutron or gamma counts per second and reported as c/s or, in accordance with standard practice, converted to parts per million or to nanocuries per gram, and in the case of soil moisture, to volume percent (vol%). Active and passive neutron and gamma measurements were made at 6-inch intervals. Raw data was converted based on calibration tests against test compositions in uniform soil or soil-like matrices. All calibration tests had been carried out by WMTS in Richland, WA. Copies of the original gamma spectrum data were also provided.

2.2 Soil Moisture Observations

A typical example of the observed soil moisture pattern[25] for most of the probe holes is shown in Figure 2.1, the soil moisture profile of Pit 9 exploratory probe hole P 908. In Figure 2.1, the volumetric moisture content increases to about 20% in the overburden at a depth of about 1.5 feet. Below 4 ft, indicating the beginning of the waste zone, the soil moisture begins to decrease, and finally in the waste zone decreases to less than 1% at a depth of 7 - 9 ft. There is then an increase to 22% in the underburden (soil) beginning at a depth 10 – 11 ft. P 908 was used as a consistency check, and the multiple curves obtained on different days indicate data reproducibility.

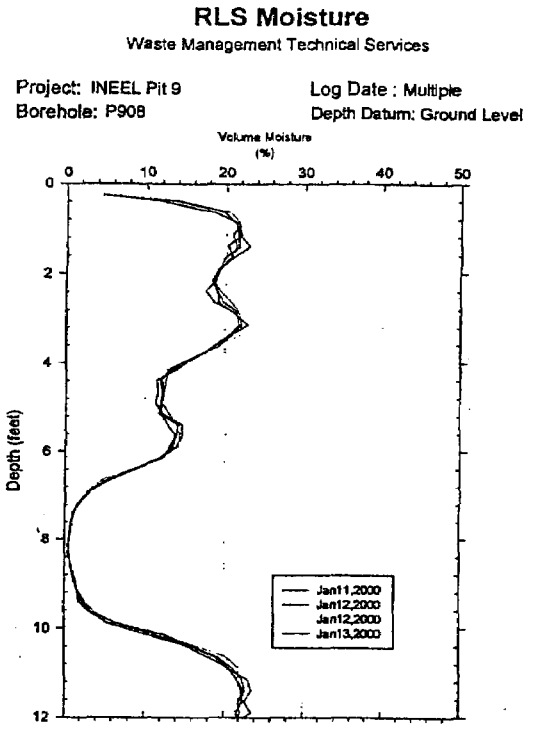

Figure 2. Composite Plot of Neutron-Moisture Repeat Surveys Conducted in Borehole P908

Figure 2.1. Representative volumetric soil moisture profile from P 908 from the Pit 9 Interim Logging Report.

Thirteen of the 20 probe holes show the general moisture profile, with depth, shown in Figure 2.1 and Figure 2.2a; of the remaining seven, six exhibit the behavior shown in Figure 2.2b as discussed in Section 2.3. Neutrons produced by a high concentration of plutonium dominate the remaining hole, P 920, and represent much more than the neutrons from the neutron moisture tool. Sixteen of the 20 probe holes show the moisture decreasing to less than 2-vol% for at least one measurement interval (6 inches). Three probe holes do not show the moisture level returning to 20-vol% at the bottom, but those probe holes appear too shallow to have sufficient underburden in which to make a measurement.

2.3 Hydrogen Content

The soil moisture curve shown in Figure 2.1 was generated from the measurement of thermalized neutrons (a.k.a. neutron-neutron measurements, so-called because a neutron source emits high-energy neutrons, which thermalize and are then detected by an adjacent detector, see Section 4.4 for details). A second neutron tool was also used, referred to as a neutron-gamma tool. The neutron-gamma probe emits high-energy neutrons and measures gammas resulting from the neutron-nuclei interactions. When neutrons are captured by hydrogen, they form deuterium and 2223 keV gammas are emitted. The count rate of these 2223 keV gammas is an indication of the local hydrogen content.

The 2223 keV gammas can be measured for an indication of the local hydrogen content. These measurements were reported as counts per second, and are labeled as "H." Figure 2.2 shows two examples of "moisture" and "H" measurements. Both of these measurements depend on the concentration of hydrogen atoms, independent of chemical form. The hydrogen may be present in the form of free moisture, water of hydration, or organic material. Both of the curves would exhibit the same functional patterns if not for geometry (of the neutron source and gamma detector, as will be discussed in Section 4.4) and absorption effects. Figure 2.2a, taken from borehole P 905, shows the "moisture" dropping almost to zero, while the "H" remains fairly constant and slightly increasing as the "moisture" is decreasing. Figure 2.2b, for P 913, shows "moisture" and "H" tracking as well, but the "moisture" does not decrease below 5.5 vol%. Six of the probe holes exhibited the pattern shown in Figure 2.2b, but in five of those, the moisture content did decrease below 5.5 vol%.

Figure 2.2. Examples of similar and dissimilar moisture and hydrogen measurements.

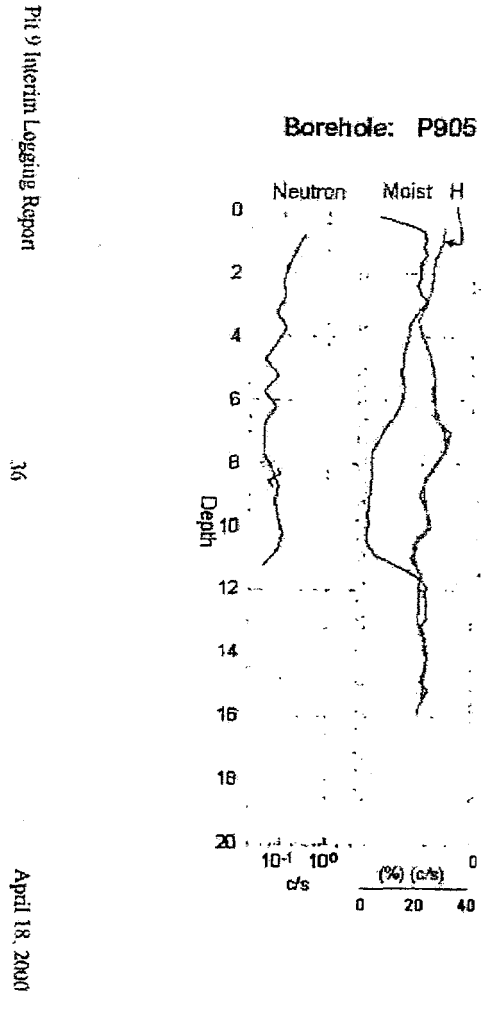

Figure 2.2a. Example where moisture and hydrogen do not track.

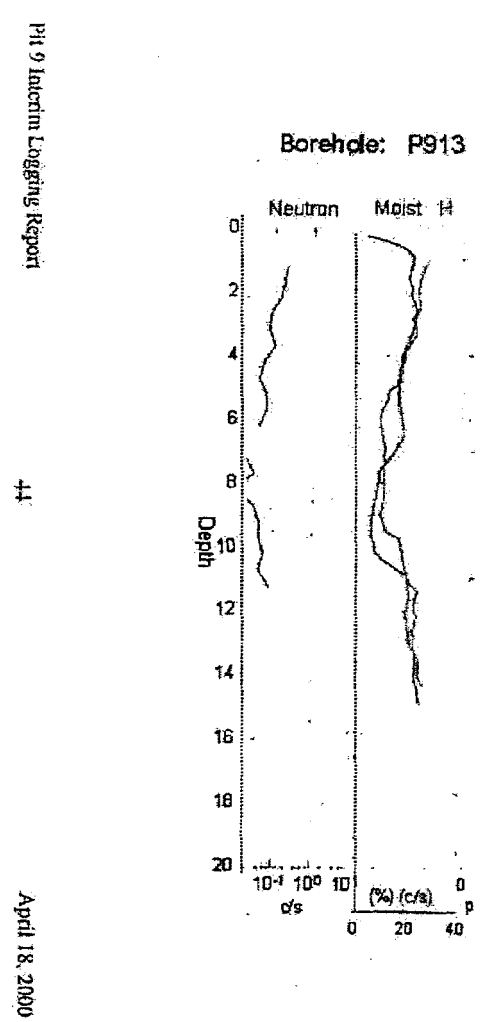

Figure 2.2b. Example where moisture and hydrogen track.

2.4 Other Observations

Other observations of interest are silicon (Si), potassium (K), and chlorine (Cl). Silicon and chlorine measurements are based on neutron capture by a silicon or chlorine atom. One isotope of potassium, K-40, is naturally radioactive and 12% of the time emits a 1460 keV gamma during beta decay. Both silicon and potassium are present in the soil. In addition, concentrations of silicon equivalent to that in the soil are expected in the Series 741, 742, 743, and 744 waste sludges. The sludges were formed in the solidification of liquid wastes by using calcium silicate and portland cement, both high in silicon. Series 745 sludge—the nitrate salt wastes—contains 30% potassium nitrate (12-wt% K) and has the highest potassium concentration of any of the waste forms. Series 745 sludge has almost no silicon. High chlorine (as much as 52-wt% Cl) is expected in the 743 sludges. These features can be used to estimate the primary waste forms that are in the vicinity of the individual measurements and possibly be used to explain the observed moisture content measurements.

2.4.1 Chlorine

One of the major waste forms disposed of in Pit 9 was the Series 743 sludge. This was a "grease-like" material produced by mixing lathe coolant (a solution of hydrocarbon oil and carbon tetrachloride), other hydrocarbons, and other chlorinated hydrocarbons with calcium silicate. Based on a representative recipe[22] that requires interpretation of "%" this waste contains at least 21.8 wt% chlorine if the "%" is assumed to be "volume percent." More recent information[9] indicates that the correct interpretation is "weight percent," in which case the 743 sludge contains 51.8 wt% chlorine, which rounds to 52 wt%, the value used in this document. From the disposal records, enough of this waste was disposed of in the Stage I subsurface exploration region to result in an average chlorine concentration in the waste zone of 10 wt%. Essentially all of the Stage I probe holes logged show measurable quantities of chlorine, as shown in Figure 2.3. The highest reported chlorine concentration was 3.5%. Chlorine has a high cross section for neutron capture and is expected to strongly influence the neutron measurements used to determine "soil moisture" content.

As shown in Figure 2.4, an increase in the measured chlorine concentration is often negatively correlated with the measured concentration of hydrogen. This indicates that chlorine reduces the available neutrons for the activation of hydrogen.

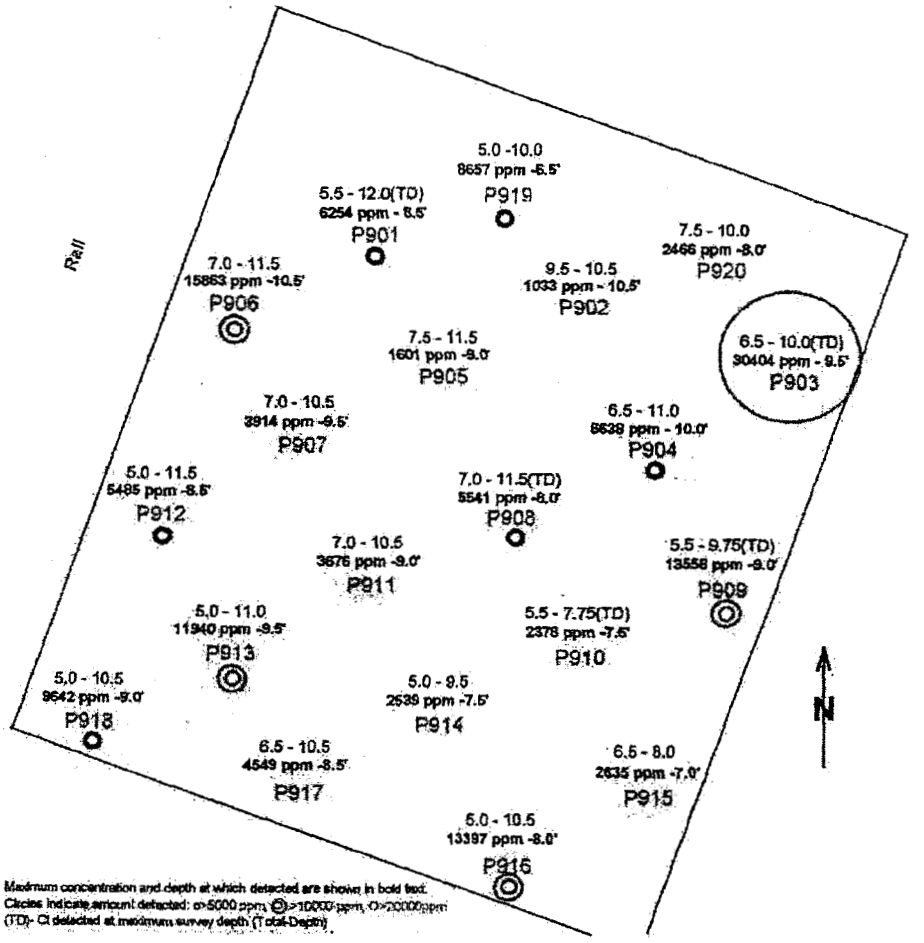

Figure 9. Chlorine Intercepts

Figure 2.3. Plan view of the probe holes showing reported chlorine concentrations (from Reference 25).

2.4.2 Potassium

Three boreholes, P 906, P 912, and P 916, show a high potassium peak (passive gamma from K-40) while at the same time showing low silicon. Figure 2.4 shows the results for P 912. These measurements are indicative of Series 745 sludge because of the high potassium and low silicon measurements. Observe that the measured K-40 concentration in the overburden and in the underburden is approximately 20 pCi/g. Both P 912 and P 916 also show the Figure 2.2b hydrogen-moisture pattern. The vertical axis of Figure 2.4 shows the full set of parameters taken from each borehole.

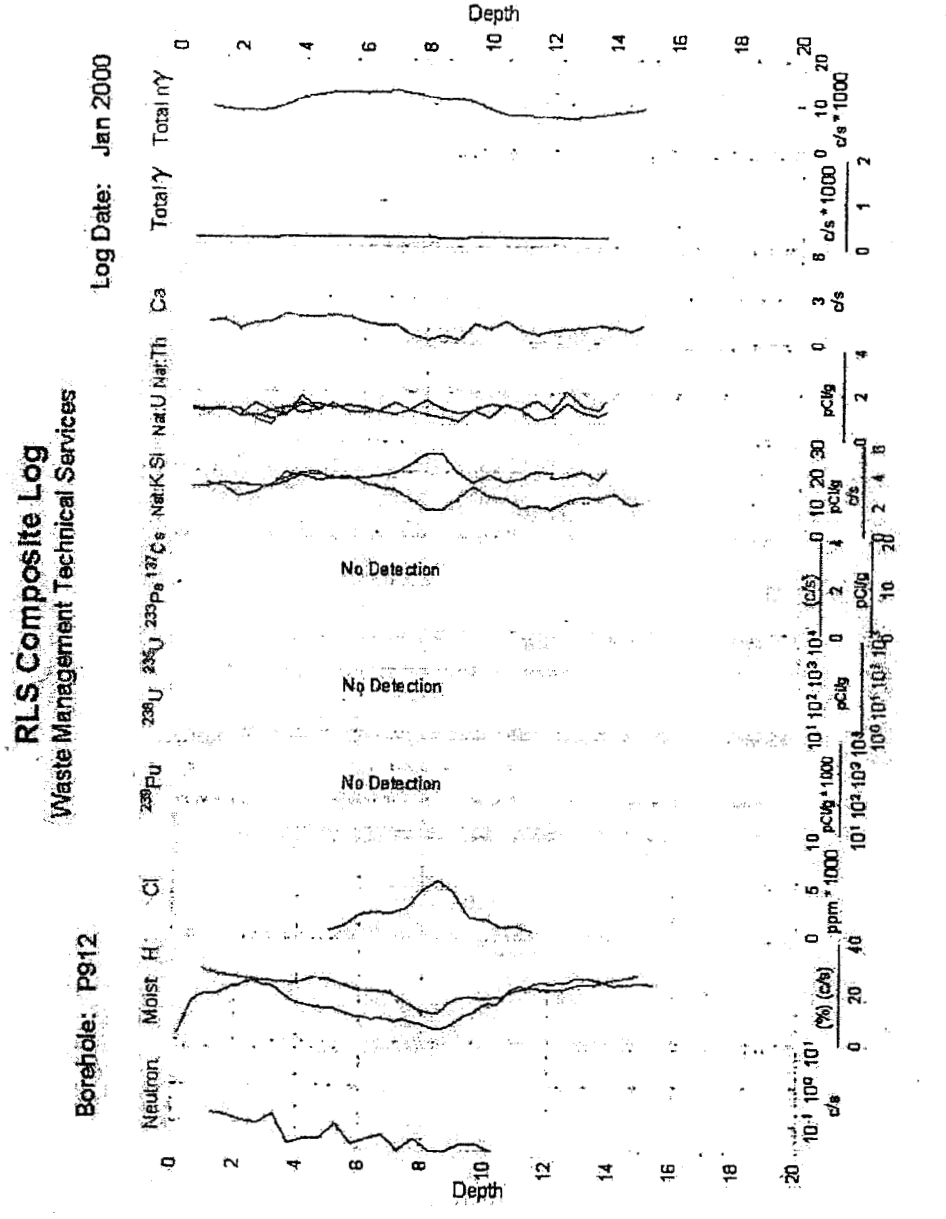

Pit 9 Interim Logging Report 43 April 18, 2000

Figure 2.4. Possible 745 sludge with high potassium and low silicon in P 912.

2.4.3 Other

Silicon measurements could also be used to judge the location of the waste zone since most waste forms have lower silicon content than the soil. The voids within the wastes enhance the reduction in silicon. However, the silicon signal was particularly weak, and so the waste zone was demarcated using moisture. No analysis of the silicon signal was performed, only the observation that the silicon signal generally decreases at a depth approximately 1 foot lower than moisture signal. Calcium was measured as well, but was found to have too little sensitivity to be of any use. Uranium was measured and found in elevated concentrations in twelve of the 20 boreholes. Plutonium and americium concentrations were measured, and are discussed in the OU 7-10 Stage I Subsurface Exploration and Treatability Studies Report,[3] but are not discussed here.

3. THE PROBLEM

The WMTS thermal neutron data collected from the initial twenty probe holes in Pit 9, based on standard soil-moisture calibration curves, show that the volumetric soil moisture content in the overburden is as expected. Between 2-ft depth and 5-ft depth, the volumetric soil moisture content is generally above 20-vol% (equivalent to 13-wt%). However, in the waste zone, many moisture level readings were well below 5-vol% (3.5-wt%).

This report evaluates the data to determine if there is a problem related to measurement difficulties or data interpretation. This report addresses these real and apparent conflicts.

Hydrogen measurements were made by using a neutron source and gamma detector to detect the high-energy capture gamma from a hydrogen atom. The moisture measurements were made by measuring neutrons thermalized by the surrounding media. The neutrons originate in an active source located near the detector (the moisture measurement tool uses a different neutron source and detector system than that used to detect hydrogen). Both tools respond to hydrogen independent of its chemical form. In most probe holes, as is shown in the behavior samples from Figure 2.2a, the hydrogen content measured via gamma rays remains fairly uniform through the overburden, waste zone, and underburden. Thus, there appears to be an inconsistency in the measurements.

Logging in some of the holes returned soil moisture content as low as 1 vol%. Achieving actual moisture contents of 1 vol% moisture in clay soils would require artificial or engineered intervention such as a drying technique. In three years of moisture monitoring at the RWMC,[5] using a neutron probe calibrated to SDA sediments, moisture contents in the clay-rich soils below the near-surface layer dried by seasonal evapotranspiration, was consistently measured above 15% by volume. In large void spaces (such as void spaces between unconsolidated waste), however, a moisture content measurement of 1% might be reasonable because few neutrons would be thermalized.

4. APPROACH

The proposed approach is to assume that the soil moisture content is a continuous, slowly varying, monotonically increasing function between the overburden and underburden. Major deviations from this model may be attributed to intact waste packages and waste forms with properties greatly different from soil. The data will be analyzed from the perspective of testing waste composition and configurations that could explain the observed behavior. The apparent decrease in indicated volumetric moisture content within the waste zone might also be explained by neutron losses due to chlorine.

Gamma spectroscopy provided measurements of chlorine, calcium, potassium, silicon, and hydrogen. These measurements may be used to identify the predominant waste forms close enough to the detector and/or neutron source to influence the measurements.

The hydrogen source may be from water, plastics, chlorinated hydrocarbons, paper, and other organics, such as the Regal oil in the Series 743 sludges.

An apparent low soil moisture content could be due to: (1) a true low soil moisture content, (2) a low density region, (3) a region occupied by large dry objects (such as rocks) or packages which were initially dry, remain intact, and preclude the entrance of moisture, (4) an unexplained loss of neutron detection efficiency, or (5) a loss of neutrons through absorption by chlorine.

The moisture measurement instrument was calibrated against a mixture of hydrated alumina and silica. The water content in this mixture was equated to the water content in a mixture of water and dry aluminum and silicon oxides that would contain the same amount of hydrogen. However, the measurement based on the calibration curve of neutron count versus moisture content must be interpreted with caution because both the soil and the waste in Pit 9 have different neutronic properties than the hydrated alumina and silica mixture.

A simple analytical approach to determine the neutronic behavior under a variety of matrix compositions is used to interpret the moisture data from neutron measurement. The approach is applied to the calibration of the instrument first. The calibration curve can be reproduced quite closely from an analytical formula with a minimum set of free parameters. This same approach is used later to interpret the moisture measurements in the soil and waste layers of Pit 9.

4.1 Equipment Description

The following section describes the five tools used in logging the Stage I probe holes. The geophysical logging subcontractor final report contains additional details concerning operation of these tools.

4.1.1 Passive Neutron Log

The passive neutron logging tool used at Pit 9 employs a 2" x 12" He-3 detector with its center located approximately 22 inches from the tool's end plug. Neutrons emitted by spontaneous fission and alpha-neutron reactions initiated by alpha emitting radionuclides in the waste are measured. At each measurement point, the passive-neutron logging tool produces a bulk count rate corresponding to the steady state neutron flux through the probe hole casing. Elevated neutron flux zones were observed in eleven of the Pit 9 probe holes. Elevated neutron flux is interpreted to indicate the presence of elevated Am-241 and/or Pu-240 levels.

4.1.2 Neutron-neutron Moisture Log

The neutron-neutron moisture tool used for Pit 9 logging incorporates a high-energy neutron source (50 mCi Am-241/Be) to irradiate the soil near the probe hole and subsequently measures thermal neutron flux at a short distance from the source. Neutron moisture tools operate on the assumption that hydrogen atoms constitute the principal neutron moderator within the soil formation and that hydrogen is present mainly in the form of water. The neutron logging tool used at Pit 9 employs a 1" x 5.2" He-3 detector with its center located 3.78 inches above the Am-Be source. The instrument output is in counts per unit time, or total counts for an interval selected to provide adequate count statistics. A calibration relationship is required to convert counts to volumetric moisture content. Calibration is a function of

source strength, detector sensitivity, source-detector geometry, well construction, lithology, and volumetric moisture content.

4.1.3 Passive Gamma-ray Log

Passive gamma ray logging involves down hole deployment of a gamma-ray spectrometer for purposes of detecting gamma-radiation emitted by spontaneous decay of radionuclides. The gamma-ray logging tool used at Pit 9 employs a 35% HPGe detector with its center located approximately 33 inches from the tool's end plug. At each measurement point, the passive-gamma ray logging tool measures the number of gamma rays as a function of energy. Characteristic gamma-ray energies are analyzed to produce estimates of specific radionuclide concentration. Radionuclides detected during Pit 9 subsurface exploration include Pu-239, U-238, U-235, Am-241, Cs-137, Pa-233, and the naturally radioactive elements potassium, uranium, and thorium.

4.1.4 Activated Gamma-ray (n-gamma) Log

Activated gamma-ray logging refers to the method whereby a gamma-ray spectrometer is combined on the same tool string with a neutron source. The neutron source produces a neutron cloud near the probe hole and the gamma-ray spectrometer detects gamma rays emitted during neutron capture reactions. Gamma-ray flux is measured as a function of energy. Certain elements (such as chlorine) that have a high affinity for neutron capture reactions may be detected based on their characteristic capture gamma-ray energies. The n-gamma tool used at Pit 9 employs a Cf-252 source (0.676 µg on 12/15/98) mounted immediately above the tool end plug and a 20% HPGe detector located 16 in from the source. Elements detected during n-gamma logging at Pit 9 include chlorine, calcium, silicon, and hydrogen. Chlorine measurements were used as an indicator for chlorinated volatile organic compounds. Calcium, silicon, and hydrogen provide information on the soil and waste matrix properties.

4.1.5 Azimuthal Gamma-ray Log

The azimuthal gamma ray logging tool consists of a gamma-ray spectrometer fitted with a windowed shield. Gamma rays incident upon the shield are effectively blocked from reaching the detector. Gamma-rays incident upon the shield window pass through the shield and are detected as a function of energy. Azimuthal gamma-ray logging is performed by rotating the detector, window, and shield incrementally around the probe hole and measuring a gamma-ray spectrum at each position. The tool permits differentiation between uniformly distributed radionuclides and radionuclides distributed as concentrated localized sources. Furthermore, the azimuth of the highest gamma-ray response indicates the direction of the localized source. The azimuthal gamma-ray tool detects the same radionuclides as the passive gamma-ray tool but at a lower sensitivity.

4.2 Calibration

The calibration information in this section is based on WMTS' calibration of their measurement tools. Their tools had been calibrated off-Site, and the moisture gauge was cross-calibrated against INEEL measurements.

4.2.1 Calibration of the WMTS Moisture Tool

The WMTS neutron moisture gauges were calibrated against silica sand and hydrated alumina standard models with known water content, located in Richland, WA. That calibration effort produced a functional relationship:

$$V = (a'C_n)^{\alpha} = aC_n^{\alpha}, \quad \text{Eq. 1}$$

$$a = (a')^{\alpha} \quad \text{Eq. 2}$$

where a and α are calibration coefficients. The calibration parameter, "a", was extrapolated from the 6 and 8-in casings used at Richland to the 5.5-in Pit 9 casing. WMTS used two separate sources identified as RLSM00.0 and RLSM10.0. RLSM00.0 was used in June 1999 when measurements were taken in the Pit 9 dogleg; it had calibration coefficients of a = 0.0000645 and α = 2.112. RLSM10.0 was calibrated November 19, 1999 and used for measurements in the Pit 9 December 1999 through February 2000; it had calibration coefficients of a = 0.0001608 and α = 2.14. The instrument was calibrated for volumetric soil moisture content up to 32-vol%. The calibration functions for the May 13, 1999 and November 19, 1999 calibrations are plotted in Figure 4.1 below.

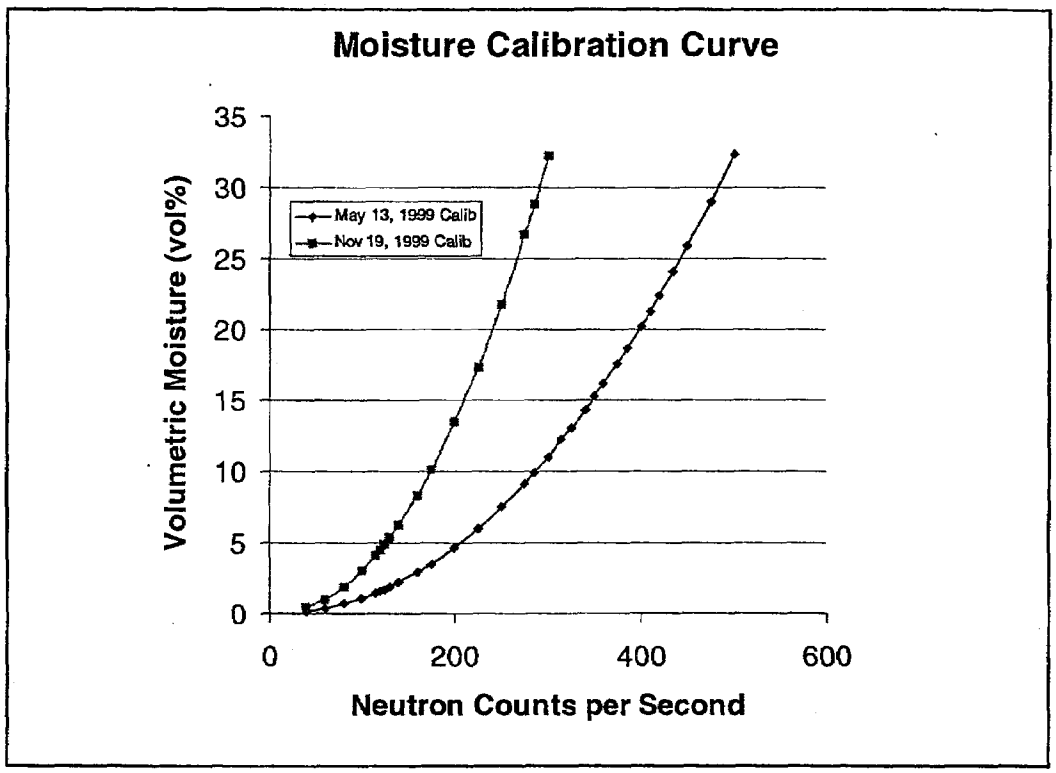

Figure 4.1. Soil moisture calibration curve generated from data provided by WMTS.

4.2.2 Cross Calibration Between WMTS Moisture Tool and SDA Measurements

On June 29 and 30, 1999, WMTS logged three neutron access tubes driven into the Pit 9 "dog-leg" to the south and east of the Stage I subsurface exploration area. No waste is buried in this "dog-leg" area. The June 1999 effort used the RLMS00.0 moisture-logging device. The peak soil moisture level measured at a depth of 2 to 4 ft in each of the holes was 16 vol%.[6]

Other moisture measurements were taken using the INEEL CPN 503 DR gauge. This gauge was calibrated to SDA soils in 1993.[5,18] To evaluate the correlation between the INEEL and WMTS gauges, in November and December 1999 they were standardized to one another using the following procedure[2]:

> Two 4-ft long, 2.5 in. OD, probe casings were hand driven, one in the Pit 9 overburden and the second adjacent to an existing 1.9 in. access tube outside of Pit 9, which had previously been calibrated to the SDA soils. Integrated Earth Sciences used the INEEL CPN gauge to log moisture in these three access tubes in accordance with INEEL practice. The neutron counts from these holes were standardized to each other, and are reported by Baker,[2] and indicate that the soil moisture between 1 ft and 3.5 ft depths varies between 20.4 and 24.3 vol%, with an average of 22.7±1 vol% moisture.

Subsequently, a 5.5 in OD probe casing was driven in Pit 9 adjacent to the hand-driven 2.5 in. OD access tube. The same procedure was repeated in December 1999 using the WMTS gauge in the 5.5-in. probe casing and the INEEL gauge in the 2.5-in. access tube. The lateral variation in moisture content within the 3-foot separation of the two access holes in Pit 9 is assumed to be insignificant. This then allows the WMTS moisture probe to be correlated against the INEEL gauge at a known moisture content. Due to the calibration methods employed, the uncertainty between the two gauges can be only judged by the difference between the measurements. The results of standardizing the WMTS gauge to the INEEL gauge was reported in Van Vliet to Beausoleil.[10] The moisture content as measured by the INEEL gauge in the 4 ft hole next to P 908 is compared to the moisture reading in P 908 taken by WMTS in Figure 4.2. The WMTS readings average 9% lower than the INEEL readings (i.e., 9% of the numerical value of the INEEL readings) at a given depth.

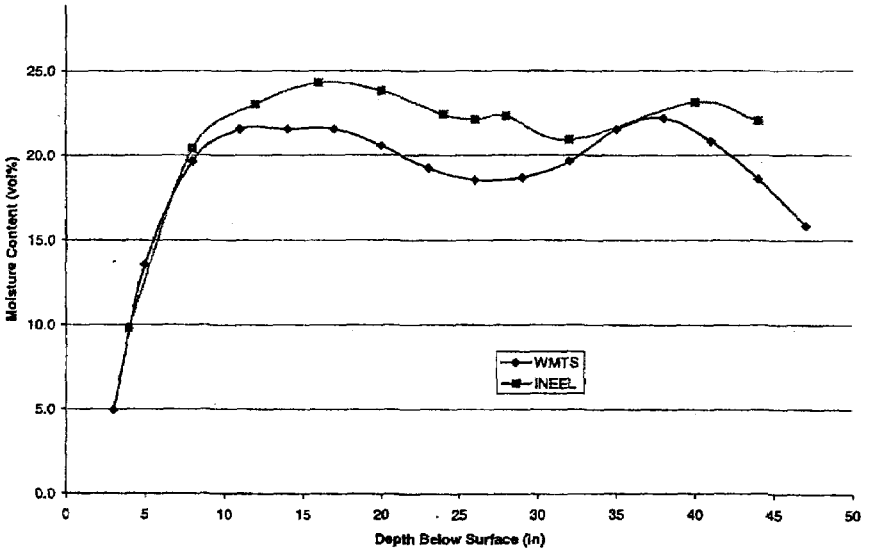

Figure 4.2. Comparison of INEEL and WMTS moisture measurements.

4.2.3 Chlorine Calibration

Chlorine calibration for the n-gamma tool was performed using a combination of physical modeling and Monte Carlo simulation. The physical model contained a 1.4-wt% chlorine standard at known density and moisture content. Calibration spectra were collected with the n-gamma tool inside the physical model. Using Monte Carlo simulation, the physical model measurements were corrected to account for the borehole size, density, and moisture conditions anticipated at Pit 9. The logging subcontractor then derived a linear calibration factor using the corrected calibration measurements for 1.4 wt% Cl and the point 0, 0 (i.e. assuming zero counts for 0 wt% Cl). The chlorine calibration utilized the 1165 keV Cl capture peak only. Statistical errors for a single measurement for the 1165 keV line is approximately 15% for a single measurement and the simulated detector response to a long cylinder is derived from 5 measurements. Therefore, the precision (repeatability) of the calibration measurement is approximately 7% (15/$\sqrt{5}$ %). The accuracy of the calibration has not been established at this time.

4.3 Waste Composition

Waste compositions in the Stage I, Phase I subsurface exploration area were studied in detail to support the Stage I, Phase II safety assessment.[4] Waste compositions were reviewed and analyzed in this study for expected volumetric concentrations of calcium, potassium, silicon, and hydrogen. The concentration of hydrogen was estimated in terms of water and organics.

The Stage I subsurface exploration area contains almost 40% (by count) empty waste drums. The influence of empty drums (air spaces) on neutron thermalization and on shielding has been only qualitatively evaluated.

With respect to interpreting volumetric moisture content, the major waste components are Cl, H, and H_2O. Each of the different waste forms has a different expected density of Cl, H, and H_2O. These have been collected and analyzed. Waste compositions were also reviewed for neutron poisons (chlorine is the only significant poison). The principal results of this analysis are presented in Table 4.1.

Table 4.1. Waste composition showing Stage I distribution, weight per drum, and estimated chlorine, hydrogen, and moisture concentration per drum.

RFP Waste Type	Number of Drums	Waste Wt[a] (lb)	Cl wt%	H wt%	Moisture wt%	Comments
Combustibles	260	116	2.5	10.1	6	1
Non-combustibles	28	104	1.0	1.1	1	2
741 sludge	3	427	0.6	5.7	51	3
742 sludge	27	339	1.5	6.7	60	4
743 sludge	379	507	51.8	2.8	0	5
744 sludge	2	312	0.0	3.1	28	6
745 sludge	42	377	2.3	0.2	1.8	7
Graphite	22	199	0.0	0.0	0	8
Empty	544	11	92.2	0.0	0	9
Soil			0.04	1.8	16	10

a. Packaging changes were made in 1970. After 1970, a 90-mil polyethylene liner was used in all TRU waste drums from RFP. Prior to 1970, the 90-mil liner was not used. Without this liner, the drums contain more waste than post 1970. Average weights in this table were obtained from actual trailer-load records. Only the density is used in this document, the actual weights are only necessary in calculating the density.

Comments

1. Estimate 11-lb polyvinyl chloride, 5-lb misc. (floor sweepings, minor laboratory items, rags), 50-lb polyethylene, 50-lb paper; paper is assumed cellulose with 10-wt% moisture.
2. Estimate 2 lb polyvinyl chloride and 6 lb polyethylene and 1% H_2O.
3. Cemented aqueous wastes containing an average of 51 wt% water.[22]
4. Cemented aqueous wastes containing an average of 60 wt% water.[22]
5. An RFP recipe reported in Schuman[22] stated that 30-gal liquid (47 vol% lathe coolant, 10 vol% trichloroethylene, 43% hydrocarbon oils and greases) was mixed with 100 lb $CaSiO_4$. About 15 lb of Oil-dry was added to each drum. We shall also assume that the drum contains 5 lb of polyethylene plastic bags. The lathe coolant was reported as 60% Regal oil plus 40% CCl_4 (it was assumed by most readers to be vol%, but was unspecified). More recently it has been concluded by Einerson and Thomas[9] that the lathe coolant is, in fact, 56.5 vol% CCl_4 and 43.5 vol% Regal oil. The Einerson and Thomas recipe for the liquid is used. It is noted that the Einerson and Thomas recipe (37 gal of liquid per 55-gal drum plus solids) would result in a drum containing 549 lbs of waste, 10% higher than the measured waste weight per drum.
6. The basic matrix is cemented aqueous wastes, the generic recipe[22] was 2 bags (94 lb each) portland cement per drum, assume 30 wt% water, i.e., 30 wt% in the grout (cement-water mix) plus the waste compounds and some plastic bagging. The average weight per drum exceeds the primary recipe by about 20%.
7. Schuman.[22]
8. Arbon.[1]
9. Assumed to be CCl_4.
10. Use average INEEL soil, 0.04 wt% Cl[17] and 22 vol% moisture.[6]

4.4 Analytical Modeling

The continuous slowing down model is used to predict the thermal neutron flux around the neutron moisture instrument. A good exposition of how this theory works is found in Glasstone and Sesonski's *Nuclear Reactor Engineering.*[12] The model assumes that high-energy neutrons created by a source are scattered to thermal energies through many collisions with the matrix nuclei until their energy distribution can be considered continuous. The model is a reasonably good approximation of neutron behavior in a matrix of heavy elements (atomic weight greater than approximately 10), but is poor in predicting neutron energy distribution in hydrogen because the neutron can lose all of its energy in a single collision with a hydrogen nucleus (proton). However, if the scattering coefficient of hydrogen is adjusted to fit the measured slowing down distance of neutrons in water, the continuous slowing down model is useful in predicting the neutron behavior under hydrogen scattering as well.

The approach used in this analysis is to first compute the slowing down distance of high-energy neutrons (energy in the MeV range) to thermal energies. The slowing down distance is represented by the Fermi distance, L_f (the square root of the Fermi age). It is then assumed that all the thermal neutrons are created at a distance L_f from the source. The thermal neutrons then diffuse and are absorbed by the medium. The distribution of thermal neutron flux is obtained by solving the one-dimensional diffusion equation. Interactions of the neutron flux with the gas nuclei in the detector give rise to electronic pulses that are counted.

4.4.1 The Fermi (Neutron Slowing Down) Length

The Fermi age, τ_f, can be calculated as:

$$\tau_f = \frac{1}{3\xi\Sigma_s^2}\ln\left(\frac{E_0}{E_{th}}\right), \qquad \text{Eq. 3}$$

where ξ is the logarithmic energy decrement per collision averaged over the macroscopic scattering cross-sections of the constituent elements of the medium, and Σ_s is the macroscopic scattering cross-section averaged over the energy range from E_0 (neutron energy at release) to E_{th} (thermal energy). The Fermi length, L_f, is the square root of the Fermi age, i.e.,

$$L_f = \sqrt{\tau_f}\ . \qquad \text{Eq. 4}$$

As described in Section 4.1.2, the neutron source consists of an alpha emitter, Am-241, and beryllium. Alpha bombardment of the beryllium results in neutron emissions with an average energy of 4.2 MeV at a rate of 65 neutrons per million alpha particles.[14] The thermal energy is taken to be 0.025 eV.

4.4.2 Thermal Neutron Flux Distribution

We assume that the thermal neutrons are created in a ring with its center at the neutron source and having a radius equal to the probe tube outside radius, R, plus the Fermi length of the medium as calculated by the formula in Section 4.4.1. The distribution of thermal neutrons in the medium outside the probe tube is assumed to be the solution of the diffusion equation for a point source in an infinite medium. If the origin of the co-ordinates is located at a point on the ring, the thermal neutron distribution arising from a thermal neutron source at the origin is given by:

$$\phi' = \frac{Q'}{4\pi D}\frac{\exp(-\kappa r)}{r} \qquad \text{Eq. 5}$$

where ϕ' is the "neutron flux" due to Q' [which is the source strength (thermal neutron generation rate) per unit length along the ring], D is the thermal diffusion coefficient, κ is the attenuation coefficient ($\kappa^2 = \Sigma_a/D$, where Σ_a is the macroscopic absorption coefficient), and r is the radial distance from the origin. The total neutron flux, ϕ, is the integral of ϕ' over the circumference of the ring.

When the above formula for the distribution of neutron flux is applied to the source-detector geometry, as shown in Figure 4.3, the following modifications are made. First, it is assumed that neutron absorption occurs only in the medium around the probe tube. Second, a constant neutron flux reduction factor is applied to the flux inside the probe tube to account for the effect of the steel tube. The fast neutron source and the detector are assumed to be located along the axis of the tube separated by a distance d. The neutron flux can be calculated as:

$$\phi = \frac{f_c Q}{4\pi D}\frac{\exp(-\kappa L_f / \cos(\theta))}{(R + L_f)/\cos(\theta)}, \qquad \text{Eq. 6}$$

where $Q = 2\pi(R + L_f)Q'$ is the total thermal neutron creation rate, and f_c is the tube correction factor. The angle, θ, is given by $\theta = \tan^{-1}[d/(R + L_f)]$ as shown in Figure 4.3.

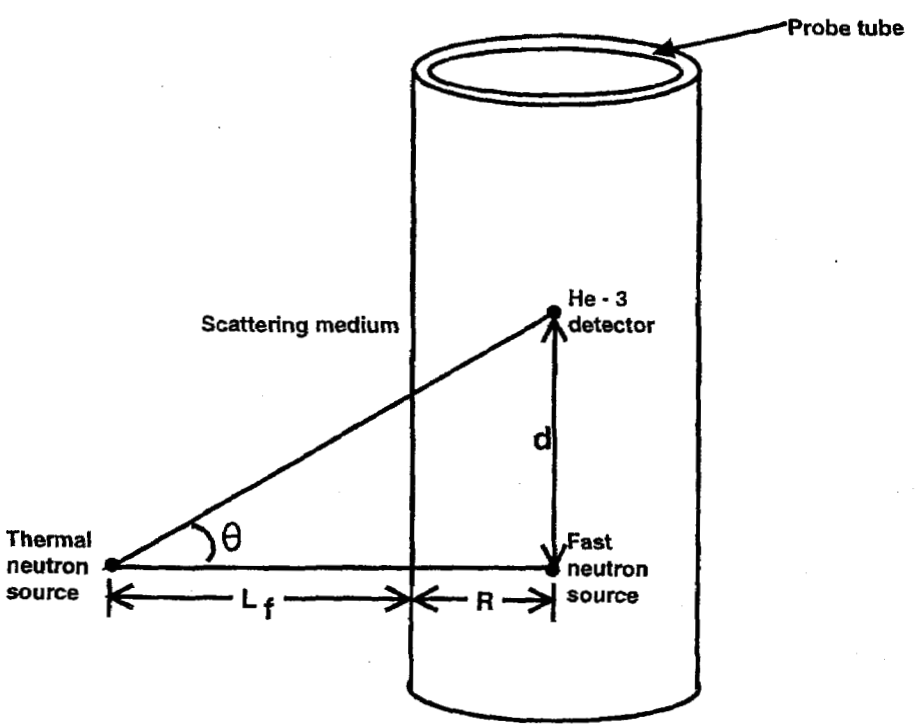

Figure 4.3. Conceptualized moisture measurement geometry.

If the detector's presence does not appreciably alter the distribution of neutrons ("optically thin"[1] or "optically thick" case), the interaction rate of neutrons with He-3 inside the detector is obtained by multiplying ϕ by the macroscopic reaction cross-section, $N_{He\text{-}3}\,\sigma_p$, and integrated over the volume of the detector. $N_{He\text{-}3}$ is the atomic number density of He-3 inside the detector and σ_p is the microscopic reaction cross-section.

The integration over the volume of the detector involves evaluation of complicated integrals. So, instead of evaluating the integral, assume that all parts of the detector are located at a distance $(R + L_f)/\cos(\theta)$ from the thermal neutron creation ring and the effective detector volume is $V\cos(\theta)$, where V is the physical volume of the detector. The thermal neutron detection rate is then given by:

$$\text{Rate} = f_c Q A(1-\exp(-N_{He\text{-}3}\sigma_p D))\frac{1}{4\pi D}\frac{\exp(-\kappa L_f/\cos(\theta))}{R+L_f}\cos^2(\theta)\ , \qquad \text{Eq. 7}$$

where A is an effective area of the detector facing the neutron flux and D is the diameter of the detector gas space. The product AD is approximately V.

The thermal neutron generation rate, Q, is only a fraction of the fast-neutron generation rate because of absorption of fast and epithermal neutrons by the medium as the neutrons scatter to thermal energies.

In the above formula the angle, θ, is a constant for a given L_f, but it also depends on the fast neutron source-detector distance, d. In order to approximate the integral over the detector volume by a point formula over a range of L_f, the fast neutron source-detector distance is used as a free parameter to fit the shape of the calibration curve. This distance should be on the order of, but not exactly equal to, the actual source-to-detector distance.

In the above formulation, essentially two free parameters are used to predict the thermal neutron count rate. One free parameter, the fast neutron source-to-detector distance, is used to approximate the reaction integral over the detector volume. Another free parameter, the thermal neutron creation rate, is used to account for the unknown absorption of fast and epithermal neutrons. This latter free parameter is related to the ratio of the thermal neutron creation rate to the fast neutron creation rate. The ratio should therefore be less than 1.

---

[1]The terms "optically thick" or "optically thin" have their origin in the behavior of visible light. Optically thick means essentially all incident photons are absorbed. Optically thin means that most photons pass through without being absorbed. It has been generalized to include the transport phenomena of any particle, and in particular, in this Section to neutrons. The parameter that determines this is $N_{He\text{-}3}\sigma_p D$. If $N_{He\text{-}3}\sigma_p D << 1$, the detector is optically thin and the expression in Equation 7 reduces to $N_{He\text{-}3}\sigma_p AD$, or approximately $N_{Ne\text{-}3}\sigma_p V$; in the optically thick limit, the expression reduces to A.

For the actual detector used in the moisture tool, the detector is close to the optically thick limit ($N_{He\text{-}3}\sigma_p D \approx 2$), i.e., almost all neutrons impinging on the detector will react with the He-3 in the gas tube. In calculating the detector response, $QA(1-\exp(-N_{He\text{-}3}\sigma_p D))$] is used as a normalizing parameter to match one point on the calibration curve, so the actual optical thickness of the detector has no impact on the calculation.

If the detector absorbs all the thermal neutrons going through the detector ("optically thick" case), the factor $N_{He\text{-}3}\sigma_p V$ in the above formula for the optically thin case will be replaced by an area approximately equal to the product of the diameter and length of the detector tube.

4.4.3 The Moisture Calibration Curve

The experimentally derived moisture calibration curve, as used to convert neutron count rates to volumetric water percentage, is given by (as discussed in Section 4.2.1):

$$V_u = 1.608\times10^{-4}(\text{Count}-\text{rate})^{2.14} \qquad \text{Eq. 8}$$

where V_u is the volumetric water percentage and Count-rate is the thermal neutron count rate in the absence of the steel tubing because the calibration is performed in a facility that does not include a casing. (Actual count rate = Count-rate $\times$ f_c, or Count-rate = actual count rate / f_c. The correction factor f_c is given by 1 / (1.311 - 0.956 $\times$ t), where t is the thickness of the steel tube in inches.) If the theory and the calibration agree, the calculated count rate ("Rate" in Eq. 7) calculated from medium properties, should be equal to the actual count rate if the detection of a reaction event is 100%.

Based on the formulation presented in Section 4.4.2, the theoretical count rates were calculated for mixtures of hydrated alumina and silica that simulate water contents up to 40-vol%. The results are shown in Table 4.2, which, in addition to the predicted measurement results of water content, also contains the neutronic scattering and absorption parameters that are calculated for the mixtures. In calculating the detector reaction rate, a fast neutron source-detector distance of 13.2 cm (actual source to detector center distance is 9.6 cm) is assumed and the constant $QA[1\text{-}\exp(-N_{He\text{-}3}\sigma_p D)]$ is set to 4.31×10^5 cm^2/s (the detector absorption is close to the optically thick limit). These parameters produce a best fit for the calibration curve. The predicted moisture measurement curve is shown in Figure 4.4.

Table 4.2. Water content prediction for mixtures of hydrated alumina and silica.

Equivalent water content of mixture (%)	Neutron slowing down length L_f (cm)	Diffusion coefficient D (cm)	Attenuation coefficient κ (cm^{-1})	Predicted count rate (s^{-1})	Predicted measured water content (%)
0	41.03	1.974	0.040	57	0.9
5	27.71	1.300	0.057	113	4.0
10	21.64	0.968	0.074	163	8.7
15	17.98	0.772	0.091	205	14.2
20	15.47	0.641	0.108	240	20.0
25	13.63	0.549	0.125	270	25.7
30	12.20	0.479	0.142	295	31.1
35	11.06	0.426	0.159	316	36.0
40	10.13	0.383	0.176	334	40.5

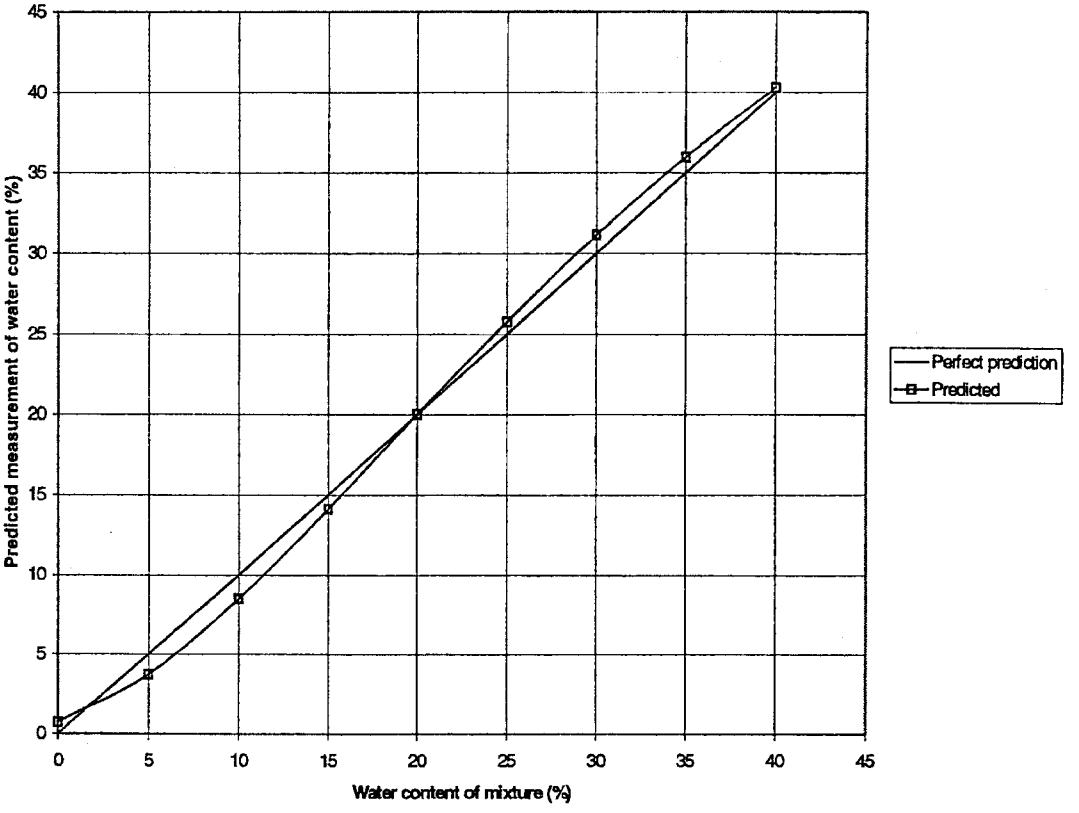

Figure 4.4. Predicted measurement of water content in hydrated alumina and silica mixtures.

4.4.4 Measurement of INEEL Soil Moisture

With the free parameters (fast neutron source-detector distance and a scaling factor for the source strength) fixed by fitting the calibration curve, predictions are made for the measurement of moisture in typical INEEL soil. The results are shown in Table 4.3 and a plot of the soil moisture content versus the predicted measurement is shown in Figure 4.5. The predicted neutron count is lower than that for the calibration model and therefore, if the same calibration curve is used, the measurement would give a lower moisture content than the actual moisture content. The main reason for the lower neutron count rate is the presence of iron and some chlorine in the INEEL soil. These elements have higher neutron absorption cross-sections than aluminum and silicon used in the calibration model.

Table 4.3. Water content prediction for INEEL soil of typical composition.

Equivalent water content of mixture (%)	Neutron slowing down length L_f (cm)	Diffusion coefficient D (cm)	Attenuation coefficient κ (cm^{-1})	Predicted count rate (s^{-1})	Predicted measurement of water content (%)
0	55.6	2.54	0.045	15	0.1
5	33.0	1.47	0.065	51	0.7
10	24.3	1.04	0.084	91	2.5
15	19.5	0.80	0.102	131	5.4
20	16.4	0.65	0.121	167	9.2
25	14.1	0.55	0.139	200	13.5
30	12.4	0.48	0.157	230	18.2
35	11.1	0.42	0.175	256	23.0
40	10.0	0.37	0.193	280	27.7

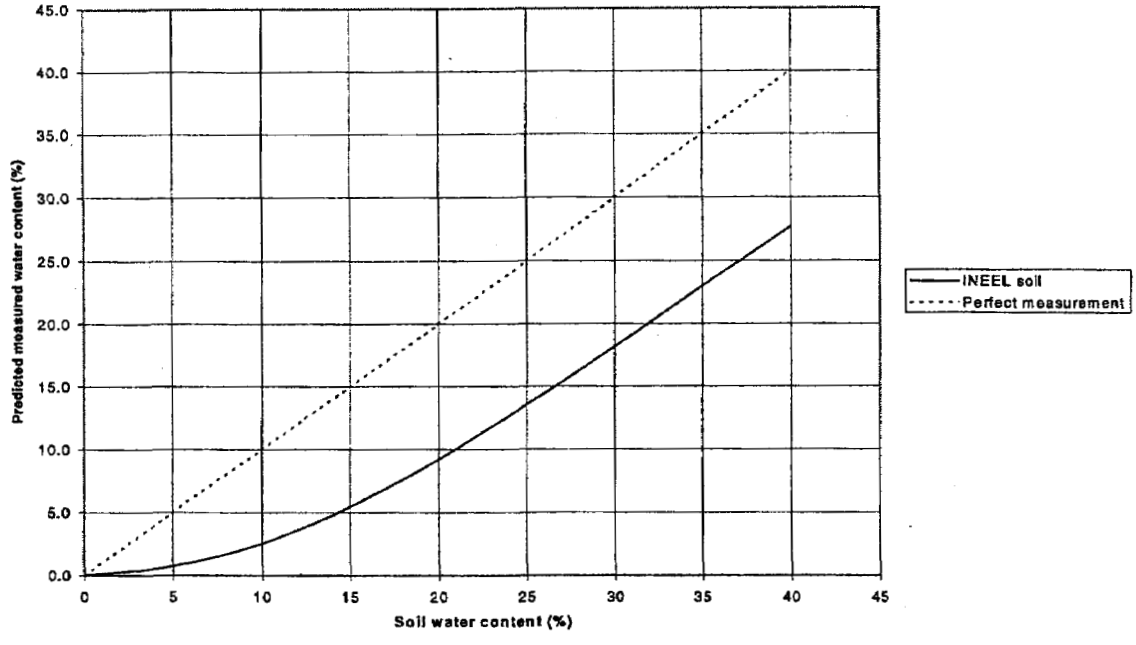

Figure 4.5. Predicted moisture measurement of INEEL soil vs. soil water content.

4.4.5 Predicted Neutron Count Rate for Various Waste Forms

Calculations were made to predict the neutron count rate for cases where the probe tube is surrounded by various waste forms. These waste forms include 74 series sludges, combustibles, and graphite. Except for the 741 sludge, which has a high content of waters of hydration, all of the waste forms in Table 4.4 are assumed to contain no significant moisture. It is recognized that this assumption only holds true if the waste containers are still intact and moisture proof. The results are listed in Table 4.4.

Table 4.4. Prediction of measured neutron count rate and moisture content (based on moisture calibration curve) in various waste forms.

Waste form	Neutron slowing down length L_f (cm)	Diffusion coefficient D (cm)	Attenuation coefficient κ (cm^{-1})	Predicted count rate (without steel tube) (s^{-1})	Predicted measurement of water content (%)
741 sludge (52 vol% moisture)	9.7	0.32	0.249	179	10.7
741 sludge (5 vol% moisture)	49.7	1.88	0.097	2.0	0.0
743 sludge	6.7	0.20	1.025	0.5	0.0
745 sludge	27.3	0.94	0.269	0.3	0.0
Combustibles	10.7	0.33	0.265	109	3.7
Graphite	10.5	0.23	0.068	2091	> 100

As can be seen in Table 4.4, the moisture content as calculated from the neutron count rate and the calibration curve bears little relation to the actual water content in the waste. For sludges and combustibles, all the moisture measurements would indicate little or no moisture. In the case of 743 sludge and combustibles, even with their high content of hydrogen, very few neutrons would be measured. The main reason for the low levels of neutrons is the presence of high neutron absorbers in the waste, particularly the presence of chlorine. In the case of graphite, because of its efficiency as a moderator and low neutron absorption cross-section, the neutron count rate is greatly enhanced to give unrealistically high water content.

Note also in Table 4.4 the range of the neutron slowing-down length, from 6.7 to 49.7 cm (2.6 to 20 in). This plus the 2.75 in. radius of the probe casing defines the nominal distance at which the neutrons can interrogate the waste, or 5.4 to 23 inches, plus the thickness of the neutron cloud. Roughly, the interrogation distance is 6 to 24 inches. Since the return gamma or neutron must pass through more than this distance to reach the detector, the true interrogation distance is more effective at the shorter lengths; furthermore, the maximum distance is only effective for the 741 sludge. It is therefore generally concluded that the effective interrogation distance is 6 to 18 inches, and for most wastes, it is only 6 to 8 inches, considerably less than a drum radius of 11 inches.

4.4.6 The Influence of Chlorine

Chlorine has a relatively large thermal neutron absorption cross-section in comparison with other elements in soil and in the waste forms buried in Pit 9. Chlorine's microscopic absorption cross-section is 33 barns, compared with only 0.33 barns for hydrogen. Because chlorine has an atomic weight of 35.5,

on an equal weight basis, it is approximately 2.8 times as absorptive as hydrogen. The presence of a few weight percent of chlorine in the thermal neutron diffusion matrix can considerably cut down on the diffusion length (inverse of the attenuation coefficient defined in earlier sections) of thermal neutrons. The neutron flux at the detector, therefore, can be reduced greatly when a few weight percent of chlorine is present. This reduction in neutron flux due to absorption mimics the effect due to lengthening of neutron slowing down length as the moisture (hydrogen) content in the scattering medium is reduced. If the moisture calibration curve in the absence of chlorine is used to calculate the moisture level based on the neutron count, the presence of chlorine in the matrix will reduce the "measured" moisture content.

Table 4.5 shows the neutronic parameters of a 743 sludge matrix. These can be compared with those for a soil matrix, as seen in Table 4.6, with 20-vol% moisture. The hydrogen content in the 743 sludge is equivalent to a matrix with 80-vol% moisture, yet the hydrogen contributes only 8.6% of the absorption; for the soil, the hydrogen contribution to absorption is 46.7%. The presence of chlorine in the 743 sludge increases the macroscopic absorption cross-section by a factor of twenty over soil.

Table 4.5. Thermal neutron absorption for a 743 sludge matrix.

Element	Mass fraction+	Macroscopic absorption coefficient (1/cm)	Fraction of total absorption
H	0.070	1.801E-02	0.086
C	0.399	9.164E-05	0.000
O	0.112	1.039E-06	0.000
Si	0.066	3.226E-04	0.002
Cl	0.260++	1.897E-01	0.908
Ca	0.094	7.291E-04	0.003
Total	1.000	2.089E-01	1.000

+This is strictly the composition of the sludge. Within a drum, there was several pounds of plastic bagging, and approximately 15 lbs of "Oil-dri" a clay absorbent.

++These calculations are based on 26% chlorine. Table 4.1 indicates a worst case chlorine level of twice this (52%). The experience of the WAG 7 vacuum vapor extraction effort suggests that much chlorine has migrated from the waste. The 26% used in this table may be low, and it may require a revision to the computations if higher concentrations of chlorine are measured at a later date.

Table 4.6. Thermal neutron absorption for INEEL soil with 20 volume percent water.

Element	Mass fraction	Macroscopic absorption coefficient (1/cm)	Fraction of total absorption
H	0.015	4.454E-03	0.467
C	0.012	3.266E-06	0.000
N	0.000	2.490E-05	0.003
O	0.562	6.127E-06	0.001
Na	0.007	1.053E-04	0.011
Mg	0.009	2.040E-05	0.002
Al	0.046	3.622E-04	0.038
Si	0.280	1.620E-03	0.170
P	0.001	3.945E-06	0.000
Cl	0.000	3.059E-04	0.032
K	0.013	6.073E-04	0.064
Ca	0.023	2.153E-04	0.023
Ti	0.005	6.219E-04	0.065
Fe	0.028	1.179E-03	0.124
Total	1.000	9.529E-03	1.000

4.4.7 Detection of Gamma Rays from Cl(n,γ) Reaction

Because the diffusion length (1/κ) of thermal neutrons in soil and in all types of waste (except graphite) is generally much smaller than the fast neutron slowing down distance, most of the thermal neutron reactions with the matrix elements occur near the point where the fast neutron is thermalized. The emission of gamma rays from these reactions can be considered as coming from a ring as at distance L_f from the outer surface of the probe tube. The count rate from a detector at a distance, d, of $Gamma_{ij}$, the jth gamma ray from element i, from the fast neutron source, can be approximated by:

$$Gamma_{ij} = \frac{Q}{4\pi((R+L_f)/\cos(\theta))^2}\frac{\Sigma_i}{\Sigma_T}s_j(BU)_m \exp(-k_m L_f/\cos(\theta))\times (BU)_t \exp((-k_t T/\cos(\theta))\varepsilon V\cos(\theta) \quad \text{Eq. 9}$$

where:

$\theta = \tan^{-1}(d/(R+L_f))$

Q = thermal neutron generation rate

Σ_i = absorption cross-section of element i

Σ_T = absorption coefficient of matrix material

s_j = number of gamma ray j from element i per absorption

BU_m = buildup factor in matrix

k_m = gamma attenuation coefficient of matrix

BU_t = buildup factor in tube wall

k_t =attenuation coefficient of tube wall

T = tube wall thickness

ε = efficiency factor (equal to macroscopic cross-section (1/length) of detector material for small detectors but, in general, depends on size of detector)

V = detector volume.

Unlike the neutron moisture instrument, the neutron gamma instrument uses a Cf-252 decay source for fast neutrons. As of January 2000 when the probe measurements were made, the fast neutron source had a neutron generation rate of 1.27×10^7 per second, with an average energy of 2.28 MeV, approximately a factor 2 lower in energy than the Am-Be source. The thermal neutron generation rate, Q, is a fraction of the fast neutron generation rate.

In this analysis, only gamma rays at the photopeak are considered. Because of the small coherent scattering cross-sections of the waste matrix and steel, the buildup factors should be all close to 1 when only gamma rays at the photopeak are considered. In other words, only the gamma rays that are not scattered or absorbed in the direct path between the point of emission and the detector contribute to the gamma count rate.

The neutronic absorption parameters are the same as those used in the thermal neutron flux computations. The fast neutron slowing down distance, L_f, is computed the same way as that used in the neutron flux calculations but using the average energy of neutrons from Cf-252 rather than from Am-Be.

As described in Section 4.1.4, the gamma detector (HPGe) is spaced 16 inches from the fast neutron source and its size is small compared to the source-detector distance. Therefore, unlike the integration of neutron reactions inside the neutron detector, the actual distance between the gamma detector and the fast neutron source is used in the computation of gamma ray counts.

In the above formulation, the only free parameter used in the computation of gamma ray counts is the efficiency factor, ε (the fraction of fast neutrons that are thermalized is also lumped into this parameter). This factor is adjusted so that the predicted counts are equal to the actual counts for a single gamma ray. The gamma ray used for this normalization factor is the 2223 keV line of hydrogen.

4.4.8 The Gamma Detector Efficiency Curve

In modeling the neutron soil moisture measurement (Section 4.4.4, Figure 4.4), it is found that the measurement, based on the hydrated alumina calibration, under-estimates the moisture content of the INEEL soil because of the presence of more neutron absorbers in the soil. For probe hole P 906 at 2 feet below the surface, the measured moisture content is approximately 20-vol%. Based on the plot in Figure 4.5, 20-vol% measured moisture translated to approximately 32-vol% real moisture content. This deduced "real" moisture content is used to compute the gamma counts rates of the 2223 keV hydrogen line. The parameter, ε, is adjusted to obtain a computed rate that is equal to the measured rate of 25.8 per second. This parameter is found to be 2.779×10^{-2} cm^{-1}. P 906 was selected above due to the extensive analysis done on this hole because of the high chlorine concentration located between 8 and 12 feet below the surface.

At the time of this writing, a calibrated gamma detector efficiency curve as a function of energy is not available. In order to correlate the gamma ray counts and the elemental concentrations for elements other than hydrogen, this efficiency curve must be known, since the gamma rays from these other elements have different energies from the hydrogen line.

In the waste zone of probe hole P 906, gamma rays from the $^{35}Cl(n,\gamma)^{36}Cl$ reaction are detected. Because of the high intensities of these chlorine lines, it is suspected that the waste form is 743 sludge. A calculation of the gamma counts of chlorine and hydrogen is carried out for 743 sludge with 10-vol% moisture, using the efficiency normalization parameter determined from the hydrogen-gamma count rate for soil. The computed count rates for a series of chlorine lines, assuming the same efficiency parameter, ε, are compared with the respective measured values. The ratios of measured counts to predicted counts as a function of energy then define the detector efficiency curve as a function of energy, normalized to an efficiency of unity at the 2223 keV hydrogen line. This deduced efficiency curve is shown in Figure 4.6. The curve is best fitted with a power law with a power index of -1.8.

The detector efficiency curve indicates that the chlorine gamma counts are consistent with chlorine concentrations over 10 wt% (see Section 4.4.9), based on the chlorine concentration in 743 sludge, except for a couple of points at the ends of the energy range. (The 787 keV line is a blend of two unresolved chlorine lines, while the 7790 keV line may be contaminated by a Ge line.) The hydrogen (2223 keV) count rate, however, is under-predicted (the measured count rate is higher than the predicted count rate).

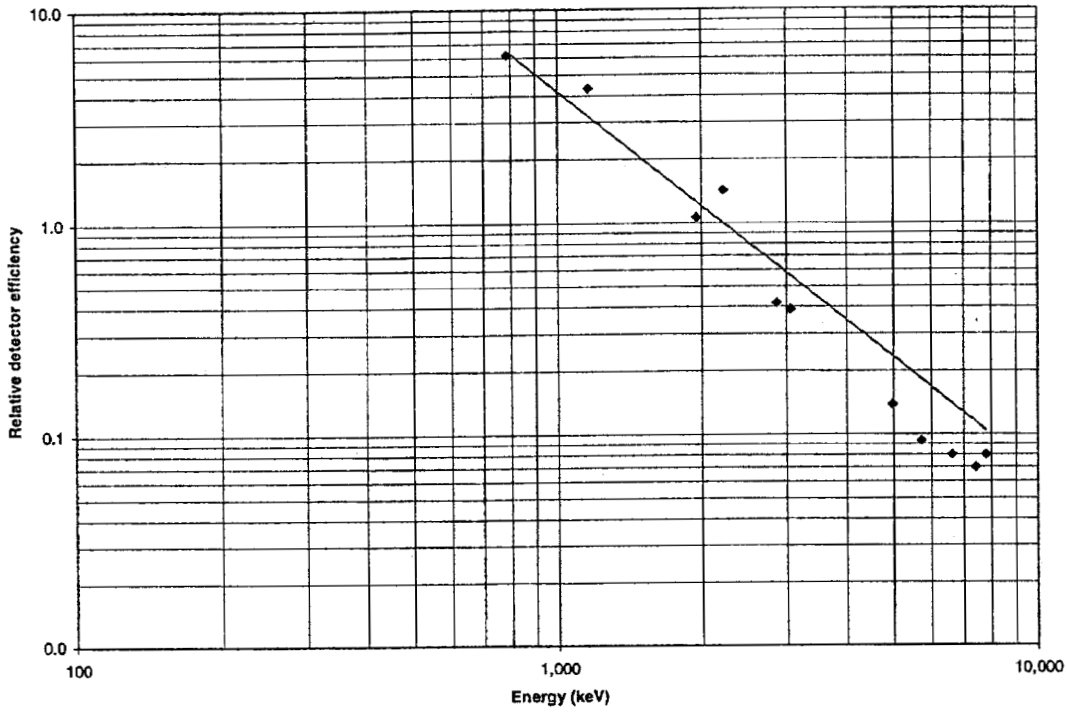

Figure 4.6. Gamma detector efficiency curve as a function of energy. The solid line is proportional to energy.[14]

The detector efficiency curve is somewhat steeper than that of a HPGe detector of similar size (the slope of such an efficiency curve is close to -1 on a log-log plot, i.e., it has a power law index of -1). The reason for this has not been determined, but it is suspected that there might be voids between the gamma-emitting chlorine and the detector, which would bring up the calculated intensities at lower energies, thus reducing the slope of the efficiency curve.

4.4.9 Gamma Intensities

The apparent success of the model to predict the intensities of measured gamma spectral lines points to the possibility of determining chlorine concentrations, and hence a signature of the waste type, particularly 743 sludge, around the probe tube based on the neutron-gamma instrument. In addition, the hydrogen gamma measurement may also provide a confirmatory measurement of soil moisture by the neutron moisture instrument. This section provides the results of predicted count rates of chlorine and hydrogen spectral lines.

Figure 4.7 shows the predicted count rate of the chlorine 1165 keV line as a function of the chlorine concentration in the waste, assuming that the detector efficiency follows the solid curve shown in Figure 4.6. The waste matrix is assumed to be 743 sludge with 10-vol% moisture, but its chlorine concentration is assumed to be a variable while the other constituents of sludge are kept constant. As shown in Figure 4.7, below 10-wt% chlorine, the count rate is fairly sensitive to concentration. Above 10 wt%, the gamma line saturates and it is difficult to infer the concentration from the gamma measurement except that the concentration can be determined to exceed 10 wt%. This curve is independent of any instrument calibration.

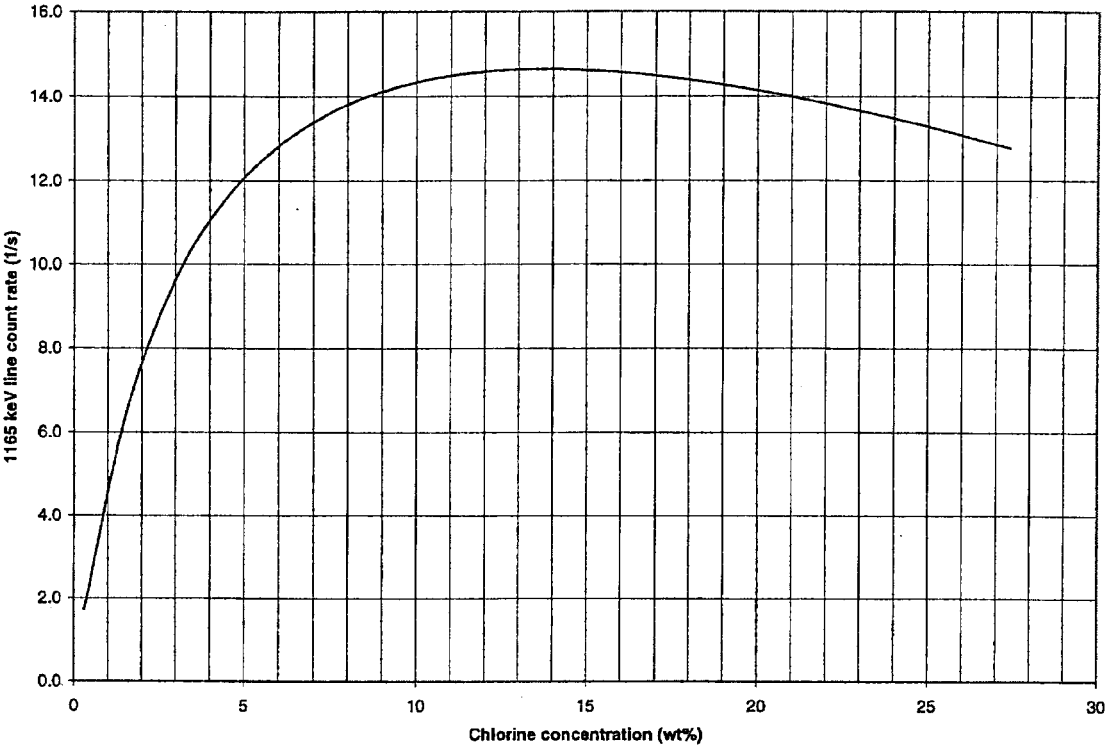

Figure 4.7. Predicted count rate of the chlorine 1165 keV line as a function of chlorine concentration in 743 sludge.

Figure 4.8 shows the predicted count rate of the hydrogen 2223 keV line as a function of the moisture content in the INEEL soil. It is to be noted that the predicted count rate is normalized to the measured count rate in probe hole P 906 at 2 ft below the surface, assuming that the moisture content there is 32 vol%, as discussed in Section 4.4.8.

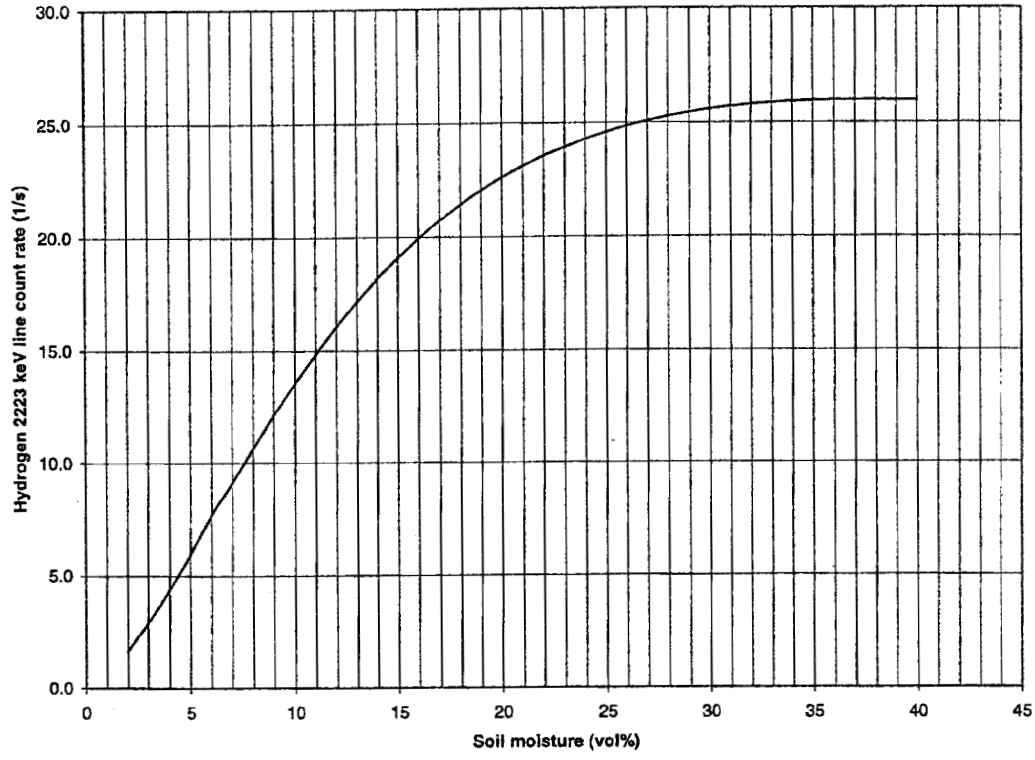

Figure 4.8. Predicted count rate of the hydrogen 2223 keV line as a function of INEEL soil moisture content.

4.5 Soil Moisture Expectations

This section evaluates the expected soil moisture profiles at the SDA in a waste disposal site.

4.5.1 Definition of Soil Moisture Content

The equation typically used in soil physics for conversion to volumetric moisture content from weight fraction of soil water (referred to as gravimetric moisture content) is defined by Equation 10.[13] The conversion from moisture content percent by weight to moisture content percent by volume is defined by Equation 11. This document refers to moisture content as the volumetric moisture content defined in Equation 10.

$$\theta_v = \theta_g * \left[\frac{(1-\theta_s)*\rho_p}{\rho_w} \right] \qquad \text{Eq. 10}$$

$$\theta_W = \left(\frac{\theta_v * \rho_w}{\rho_b + \rho_w * \theta_v} \right) * 100 \qquad \text{Eq. 11}$$

Where,

θ_v = volumetric moisture content (volume water/total volume)

θ_g = gravimetric moisture content (mass of water/dry mass of soil per unit volume)

θ_s = saturated moisture content - mass water/total volume (related to porosity)

ρ_p = particle density - assumed to = 2.65 g/cm^3 (mass soil/soil volume)

ρ_w = density of water - assumed to = 1.0 g/cm^3(mass water/water volume)

θ_W = percent moisture content by weight (mass water/mass total*100), and

ρ_b = soil (or sediment) dry bulk density (mass soil/total volume).

The above definitions are true for a homogeneous media. In the case where there are solid surfaces or voids, water may "wet" the solid surface if water is available and if the surface attracts water, but the void spaces may remain dry because the capillary forces (matric potential) may not be sufficient to maintain water in the voids.

4.5.2 Expected Pit 9 Soil Moisture Configuration

Pit 9 was backfilled with six feet of soil that is generally free of waste. The initial two feet of backfill (now lying 4 to 6 feet below the surface) was soil removed to form the pit. The top four feet of soil came from the nearby Spreading Area B, as did much of the SDA backfill. The properties of these soils have been extensively studied.[8,15,17,23] The underburden is probably 1 to 4 feet of undisturbed soil, typical of the undisturbed soils at the SDA. The soil moisture measurements in the overburden and underburden are quite consistent and generally between 20 and 25 vol% except in the upper surface layer. The moisture in the top 2 and a half feet of soil may be wetter or drier than the deeper soil depending on the season. Additionally, the upper surface layer in the Stage I area was influenced by the presence of a geofabric cover placed shortly after the spring thaw and a rainy spell. In the top foot above the waste, accurate moisture measurements are impossible because of the influence of the waste zone. The waste lies between the overburden and underburden, 6 to 12 feet beneath the surface. The expected moisture content in the waste zone is modeled below based on known moisture-transport behavior. The moisture may move within the soil independent of the waste, or it may interact with the waste.

4.5.3 Influence of Pores

Soils consist of a solid skeleton (matrix) with pores in between. The pores have different sizes, shapes, and spatial distributions, and provide the space for storage and transport of soil water. Storage or retention of water by soils is a result of attractive forces between the solid and liquid phases. These "matric" forces enable the soil to hold water against forces or processes such as gravity, evaporation, uptake by roots, etc.

The amount of water retained at relatively low values of matric suction depends primarily upon the capillary effect and the pore-size distribution, and is strongly affected by the structure of the soil. At higher suctions, water retention is due to adsorption and is influenced less by structure and more by the texture. For example, the greater the clay content, in general, the greater the water retention. However, in sandy soil, most of the pores are relatively large, and once these large pores are emptied at a given suction, only a small amount of water remains.

Void spaces in the waste materials are likely to be quite large (larger than void spaces between sand particles) and will be emptied of water. However, in areas where soil is mixed with the waste, the soil is likely to be moist due to its high clay content associated with its small pore spaces and fine texture.

In 1996, an engineered barrier test was conducted near the SDA.[21] A layer of soil was covered by a 3-ft layer of 8 - 10 inch river rocks, which in turn were covered with 4-ft of soil. The soil was obtained from Spreading Area B, which was the same source as the Pit 9 overburden. After the layered structure had been completed, neutron-neutron soil moisture measurements were made. The result is shown in Figure 4.9. It shows an upper layer approximately 16-vol% and a lower layer, which increases, to 22-vol%. The rocks contain essentially no water other than soil that has fallen into the voids between the rocks (although the barrier construction has attempted to keep the rock zone soil-free). The moisture measurement indicates 6 - 7 vol%. This is exactly the pattern expected in a waste zone if it were not for other factors.

Figure 4.10 is the moisture profile expected through the waste. Figure 4.10 was reported in 1996 as a part of a landfill closure demonstration project.[16] A mock-up similar to Pit 9 was constructed using surrogates, non-hazardous, non-radioactive materials, but otherwise representative of what was disposed of in the Stage I area of Pit 9. Following the emplacement of surrogate wastes, a neutron access tube was driven through the overburden, wastes, and underburden. Soil moisture was then measured as shown in Figure 4.10. The soil moisture profile in Figure 4.10 is as would be expected as a result of change in matrix composition in the absence of strong neutron absorbers. Since there is no chlorine at this site, the apparent moisture drops to approximately 7-vol%, which can be explained in terms of voids too large to hold moisture in an unsaturated matrix. The peak at approximately 5-ft corresponds to an elevated hydrogen content in the soil layer located between waste levels 1 and 2. The elevated hydrogen probably results from a combination of increased moisture in the soil and the clays themselves, which have hydrogen bound in their matrix.

4.5.4 Soil Description

The calcium, potassium, and silicon signatures can be used to estimate the amount of soil present. This estimate of the amount of soil may be corrupted by the presence of calcium, potassium, or silicon in the waste. The calcium, potassium, and silicon signatures have been reviewed for consistency with the expected composition of soil and soil combined with expected waste forms. Martin[19] provides the results of detailed measurements of metals and radioisotopes in soils from the INEEL and surrounding areas. Low[17] provides sampling results which show the anion content in RWMC soils. Additional soil descriptions may be found in Stephens[8] on soil hydraulic properties, and in Lee[15] and Shaw[23] on soil composition. The signal strength (counts per second) from calcium was too week to make use of. The silicon and potassium signals were of sufficient strength to determine the location of the waste. The potassium signal is strong enough to detect the location of the 745 sludge drums.

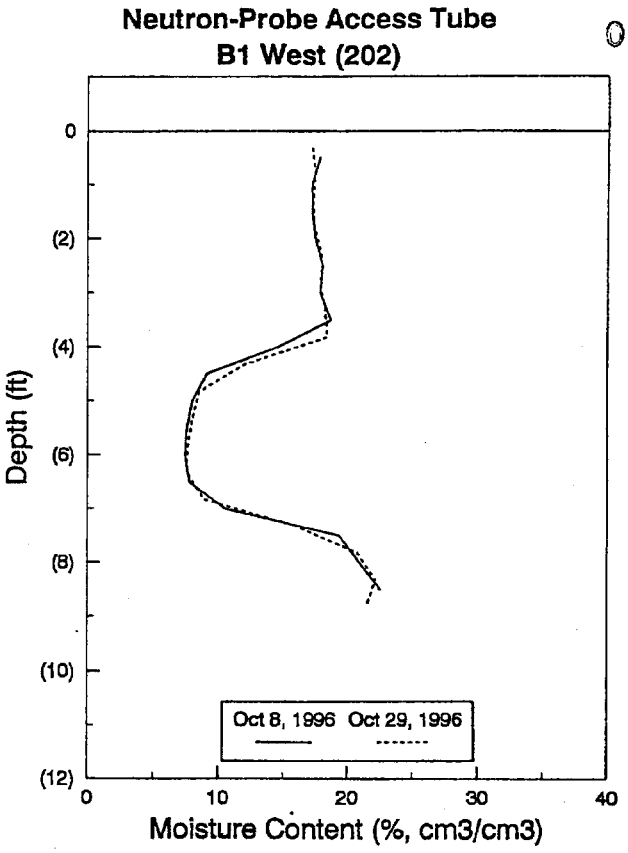

Figure 4.9. Contrasting moisture behavior in soil with river rock interbed.

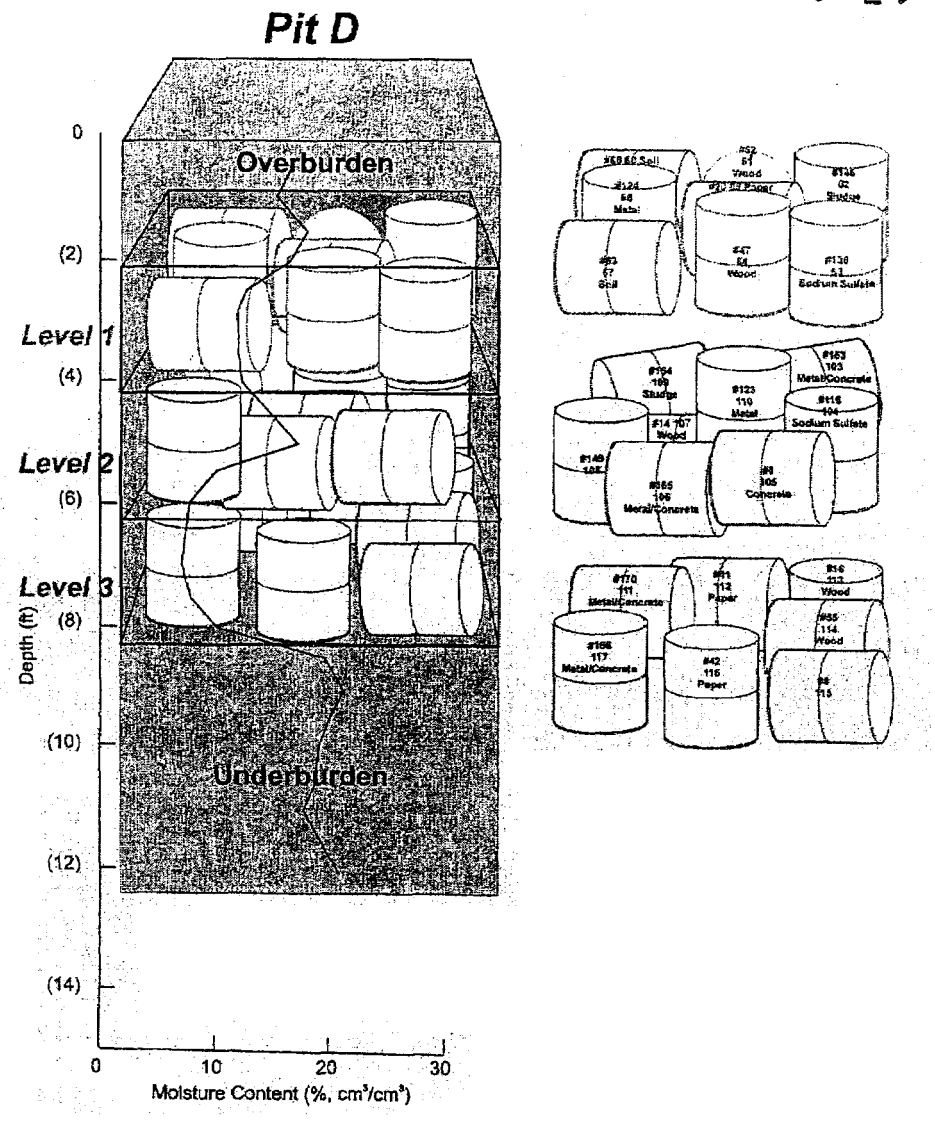

Figure 4.10. Soil moisture behavior in cold test pit.

4.5.5 Moisture Behavior in Interstitial Soils

There are large variations in the physical properties of the waste medium, which consists of wood, steel, soil, solid waste, liquid waste, and void space in a rather random arrangement. These variations preclude the conventional interpretation of in-situ, neutron-neutron moisture measurement techniques, which are based on homogeneous matrices. The results of the neutron probe can be interpreted in a variety of ways, all of which may be technically defensible. Some additional insight into the moisture conditions within the waste medium can be obtained from understanding soil humidity and matric potential.

Neutron probe measurements consistently show 20 - 25 vol% moisture within waste overburden soils and 23 - 32 vol% moisture within waste underburden soils. The highest moisture content, 32-vol%, was measured in P 918, the deepest of the probe holes, allowed moisture measurements to 17.1 ft deep.

These moisture content values are considered accurate since they agree with theoretical calculations and neutron access tube measurements made within the SDA independent of this project.[6] The 3 - 5 ft thick overburden soil layer and the 0 – 4 ft thick underburden soil layer form continuous boundaries above and below the waste zone except for isolated areas such as may exist in P 910. In P 910, refusal was encountered at 9.5 feet. The depth at which chlorine was detected in adjacent holes was 10 feet, and therefore the presumed maximum depth of waste, implies that, in this instance, the waste may rest directly on basalt. The overburden and the underburden therefore provide significant moisture reservoirs above and below the waste.

Water within soil is present in thin liquid films distributed over the surface of individual soil grains, e.g., see Figure 4.11 (from Freeze and Cherry[11] Figure 2.12). The vadose zone by definition is unsaturated, with intergranular pore spaces containing air. Equilibrium exists between the gases dissolved in the liquid films and the pore water vapor. Barring rapid temperature changes, pore space water vapor pressure remains in continual equilibrium with liquid pore water. If surface tension is neglected, this equilibrium vapor pressure, called saturation humidity, is only a function of temperature. The saturation humidity at 10°C is 9.4 g/m^3. As the temperature rises or lowers in response to seasonal or climatic temperature changes, water molecules move between the liquid and vapor state to maintain saturation humidity.

Figure 2.12 Groundwater conditions near the ground surface. (a) Saturated and unsaturated zones; (b) profile of moisture content versus depth; (c) pressure-head and hydraulic-head relationships; insets: water retention under pressure heads less than (top) and greater than (bottom) atmospheric; (d) profile of pressure head versus depth; (e) profile of hydraulic head versus depth.

Figure 4.11. Groundwater conditions near the ground surface.[11]

Saturation humidity is a smoothly varying, continuous function of position. Any local pockets of "dry" air would be quickly moistened by the movement of water vapor through the network of pore spaces in response to pressure gradients. Likewise, water vapor pressure within waste zone pore spaces will eventually reach saturation humidity. This diffusion process requires a finite amount of time. Two conditions at Pit 9 suggest that the vapor pressure within the waste zone is currently at saturation humidity.

- Temperature within the soil zone has minimal seasonal variation (the annual variation at 7 ft depth is about 20°C and at 13.5 ft depth is at only about 4°C).[7,24]

- Overburden and underburden soil moisture, which has been monitored at the SDA for 15 years, has provided a continuous water reservoir to maintain saturation humidity.

The impact of the observed flooding events at the RWMC may not have resulted in large-scale saturation of the surficial sediments. Water generally ponds in low areas and infiltrates in localized areas under the ponds. If the surface sediments are frozen when the flooding occurs, the above process is accentuated. In other words, most of the water redistributes to low areas where it collects until the subsurface thaws sufficiently to allow infiltration. When thawing occurs, the water moves rapidly through preferred pathways into the subsurface. Little is lost to evapotranspiration, because in the early spring evaporation is slight and plants are dormant

We may, therefore, estimate the vapor pressure and saturation humidity within Pit 9 waste zone pore and void spaces based on temperature. This prevailing pressure and humidity will dominate the pore space throughout the waste volume, overburden, and underburden. Some amount of water vapor will be deposited as liquid water film on the pore or void space walls under the influence of the matric potential (or tension head) exerted by the media. Since matric potential increases in inverse proportion to grain size, this effect will be greater for fine-grained media such as silt or clay than for coarse-grained media such as gravel, boulders, or macroscopic objects like waste containers. In any event, the liquid-vapor system will continually re-equilibrate by influx of water vapor from overburden and underburden soils via the interconnecting pore network until a steady state is achieved.

The amount of liquid water deposited in this manner depends primarily on temperature, grain size, and porosity. Soil masses intermixed with containers and debris within the Pit 9 waste zone will have grain size and porosity commensurate with overburden and underburden soils. It is therefore reasonable to expect that under saturation humidity conditions, moisture content within these waste zone soil masses will be approximately equal to moisture content within over- and underburden soils, or approximately 20 - 28 vol%.

Water content near containers or other debris cannot be easily estimated, but the concept of water content itself breaks down under these conditions since it depends heavily on the choice of sample size and position.

It is worth noting that hydrologic phenomena other than "film flow" as described here may contribute additional moisture content to the waste zone. Gravity flow and infilling of water into local pockets may also occur. The film flow case therefore provides a minimum water content estimate.

4.6 Equilibrium Moisture Content

Materials, which exhibit hygroscopicity, will absorb water until they reach a state of equilibrium. At that point, the moisture content (by weight) is known as equilibrium moisture content. The

equilibrium content is dependent on ambient temperature, humidity, whether the water is absorbed via gas exchange or liquid contact, and/or chemically attached as in waters of hydration.

Data for water absorption in solids is usually obtained in industrial systems when wet materials are dried. There are several parameters in the drying process including the equilibrium moisture and critical moisture content. Critical moisture content is that point in the drying process, at a given drying temperature, where the water removal-rate exhibits a sharp decrease. Equilibrium moisture content is the amount of moisture that a material will take on at a given temperature and humidity. Since the drying process is generally at slightly elevated temperatures, the equilibrium content is expected to be higher than the critical moisture temperature, although they may be nearly equal. Few standard values exist since they are specific for each solid, process, and condition.

The value given for critical moisture content obtained from chapters 20-22 of *Perry's Handbook of Chemical Engineering,*[18] is above 16-wt% for potassium nitrate. Although the temperature is not specified, the text implies a temperature of 25°C with a caveat that equilibrium moisture content is essentially independent of temperature between 15 and 50°C. As discussed below, given sufficient container breaching to allow either direct water influx or measurable vapor transport into salt wastes, alkali nitrate salts should equilibrate to at least 16-wt% moisture.

The RFP salts originated as a saturated solution that was "dried" to give a salt cake with a moisture content estimated by operators to be less than 25 wt%. The actual as-manufactured moisture content was not measured or controlled and is mostly anecdotal. Based on reports from plant operators, the solid alkali nitrate salts had no free liquid when they were packed and "extra energy" was generally provided to ensure a dry, freely flowing product.

As much as 40 pounds of portland cement, 10.6% of the final waste mass (as shown in Table 4.1) was added both under and on top of the salts. The function of the cement was to eliminate free water that might be released as the salts were cooled, handled, and transported. The cement would also force the moisture content considerably below the 16% equilibrium value, because portland cement has a higher affinity for water than nitrate salt and absorption of water by dry portland cement is irreversible. Portland cement can incorporate up to 30% its weight in water and thus this amount could theoretically remove an additional quarter of the remaining water in an initial 12% moisture salt cake.

The above-mentioned "initial" moisture-content, <25 wt%, is from operators reports when the drying process was initiated and while it was being perfected; it is not a quantitative nor substantiated.

The drying process improved in the 70's with newer drum dryers. After 1970, nitrate salts shipped to the INEEL were stored on Pad A. There the drums and boxes of salts are stacked on the surface on an asphalt pad. Closure of Pad A, which occurred in 1978, consisted of covering the stacked drums with plywood and plastic followed by three or more feet of soil.

A drum initially stored in 1972 or 1973 was retrieved from Pad A in 1988. The retrieved drum had exterior rust and a pinhole leak. Though the drum thickness were such that it could still be classified as acceptable for shipment it was placed in an 83 gallon overpack. The drum remained in the overpack until its contents were sampled in 1992.

The drum was difficult to open due to the rusty lid but the two plastic bag liners were both supple and intact. Samples taken from the drum were loose and flaky on top and dense and clumped on the bottom. Composite samples of nitrate salts were visually dry. The only evidence of moisture was the solidification of the cement and the fusing of the nitrate salts in the bottom third of the drum. The portland cement in the drum was hydrated under the salts and not hydrated on the top of the salts. This

indicates that some moisture was absorbed by the cement but that the moisture reducing properties of the portland had not been exhausted.

Water content within the drum varied by 1%. Water content of the composite samples measured in 1992 and 1999 was 2.2±0.4 wt%. It is likely that most of the drums on the Pad contain equally dry salts and that most of the buried salts in drums that still have sealed plastic bags will have moisture contents under the critical moisture content. Furthermore, based on the above observations, it is reasonable to expect that many of the salt drums buried in Pit 9 are still sealed (that is the plastic bags are sealed, as they were at the time of packaging) and thus have depressed moisture levels.

It is expected that 100% (saturation) humidity exists within the waste zone containing the nitrate salt drums. Peak overburden and underburden measurements indicate 20-28 vol% soil moisture.

Saturation humidity within salt waste pore spaces can be reached by direct influx of water or by water vapor flow through interconnected pore spaces in surrounding soils if the drum and plastic bagging is breached.

Given sufficient drum breaching, the amount of water deposited in salts from water vapor in soil depends then on temperature, grain size, and porosity. In the extreme case where soil itself is intermixed with the salts, the grain size and porosity are probably the same and saturation humidity conditions would then be 20 - 28 vol% (14 to 16 wt%).

Additional moisture can enter the waste salts from gravity flow and infilling of water into local pockets. The diffusion of water vapor therefore provides a minimum water content estimate.

In summary, the moisture content of the nitrate salts is expected to be as low as 2-wt% and no more than 12wt% for drums in which the plastic bagging is intact. The final water content, however, of the waste salts, and any change content from the initial amount as packaged, primarily depends on the degree of container breaching. Breached drums with breached bags will be in equilibrium with the soil vapor phase and near or above the equilibrium moisture content of 16-wt%.

5. EVALUATION

Evaluation of the Stage I logging data leads to the following understanding of the Pit 9 subsurface exploration area.

5.1 Soil Moisture

Counting thermalized neutrons provides an accurate measure of soil moisture content when the media is known and the neutron moisture tool is calibrated against the soil. Since significant levels of confounding contaminants (chlorine or neutron-producing radioactive materials) were not observed in the overburden, it can be concluded that the observed soil moisture measurements in the overburden are valid. "Significant levels," defined from the tables presented in Section 4.4.6. The absence of those contaminants was confirmed by n-gamma passive gamma logging measurements. Similarly, the soil moisture readings in the underburden, once out of the range of the waste zone, are valid.

The WMTS logging tool was cross calibrated against a 4-ft probe casing hand driven adjacent to P 908; a similar 4-ft probe casing was hand-driven adjacent to a separately calibrated neutron access tube outside of Pit 9. This enabled the validation of the soil moisture measurements in the overburden. The volumetric soil moisture content as a function of depth in the overburden and underburden closely approximates the soil moisture content in the SDA outside of Pit 9.

Except for the near surface soil, less than three feet deep, soil moisture in the overburden and underburden is unsaturated and is consistently in excess of 20-vol% but less than 28-vol%. At depths less than 3 ft, the moisture content is seasonally dependent, as well as influenced by the geofabric covering of the Stage I subsurface exploration area.

Based upon the arguments presented in Sections 4.5 and 4.6, it is believed that the interstitial soil has a moisture content equivalent to that of the overburden and underburden, between 20 and 26 vol%.

5.2 Moisture Measurements in the Waste Zone

The neutron moisture-logging tool clearly identifies regions in which the matrix contains material other than soil. This is due to not only the change in moisture content, but also the presence of voids and chlorine, which affect the apparent moisture content. The neutron moisture logging tool was used to determine the location of the waste zone with a fair degree of accuracy, within approximately 1 foot (additional details are published[3] elsewhere and are not repeated in this report).

Thus, it was expected that the apparent soil moisture content might have decreased by a factor of two because of voids and large waste forms as shown in Figure 4.10. Alternatively, apparent moisture content might have increased by a factor of four, if embedded in a high-density hydrocarbon oil containing waste form. Instead, decreases to effectively zero were observed. This report has shown that this apparent decrease in moisture content can be qualitatively attributed to the presence of chlorine.

A theoretical model was utilized to predict the neutron count rate that should be measured when the probe is surrounded by various waste forms. The model is based on the geometry and physical parameters of the WMTS neutron moisture-logging tool. As was shown in Table 4.4, the neutron count rate predicted by the model bears little relation to either the hydrogen or the moisture in the waste. The principal reason for this is not only neutron absorption by chlorine but neutron absorption by other elements. Alternatively, for graphite, a waste form present in 3 to 10% of the drums, the predicted neutron count rate is greatly enhanced and will produce an unrealistically high water content.

The model can be used to qualitatively explain observed neutron moisture observations. If there is a high chlorine reading in the same location, it is obvious that the soil moisture reading will be low, independent of the local hydrogen content.

It is therefore concluded that it is impossible to use the thermal neutron moisture probe to determine moisture content in the waste zone.

5.3 Chlorine

Chlorine is measurably present in the waste zone. It was reported by WMTS at concentrations between 1,000 and 30,000 ppm (0.1 to 3-wt%). Chlorine has a high cross section for neutron absorption and therefore impacts the apparent moisture, chlorine, and hydrogen measurements, as demonstrated in Section 4.4. Upon evaluating the behavior of neutrons in the presence of chlorine, it is obvious that calibration of gamma counts to chlorine concentration may be low by as much as a factor of 10. It is concluded that the conversion of chlorine n-gamma measurements to chlorine concentration at this time was not accurate due to the initial calibration range. Additional calibration using a test medium with neutron response properties closely resembling 743 sludge is required before the existing measurements can be properly interpreted. Since the 743 sludge is the only waste form with chlorine content in excess of 2.5 wt%, accurate readings only above 5-wt% are required to determine the presence of a 743 sludge. However, if it is desired to establish the presence of the as-packaged chlorine content, then, it will be necessary to calibrate at chlorine levels at least to 25-wt%, preferably as high as 50-wt% chlorine.

5.4 Hydrogen

The mass fraction of hydrogen in the combustible and Series 741, 742, 743, and 744 sludge wastes exceeds the amount of hydrogen expected in the soil at 20-vol% by factors of 4 to 6. The hydrogen in the combustible wastes arises from plastics and paper present. The hydrogen in Series 743 sludge arises from hydrocarbon oil (Regal oil). In the other sludges, the hydrogen is from water of hydration in the cemented waste forms. Thus, there are reasons to expect that the measured moisture content could have either decreased or increased, but in no case decreased to less than 1-vol%. The apparent soil moisture content might have decreased by a factor of two because of voids and large waste forms as shown in Figure 4.10. Alternatively, the soil moisture readings might have increased by as much as a factor of six, if taken inside a high-density hydrocarbon oil containing waste form. Instead, decreases to effectively zero were observed. The analysis in Section 4 shows how this decrease can be qualitatively attributed to the presence of chlorine.

The hydrogen concentration was independently determined from the intensity of the 2223 keV gamma line using the n-gamma tool. This tool more closely measures the hydrogen concentration less dependent on but still impacted by the local chlorine concentration.

5.5 Waste Zone Soil

Active gamma lines from silicon and passive gammas from potassium-40 were measured.

The measured gamma signal from silicon qualitatively shows a decrease within the waste zone. However, the silicon gamma was of little value as either a waste zone marker or a measure of the relative amount of interstitial soil within the waste zone because it is weak and affected by the presence of chlorine.

The potassium-40 signal is from the naturally occurring K-40 isotope. The INEEL soil contains approximately 2400 ppm(mass) of potassium and with 22±4 pCi/g of K-40.[19] Except for the 745 sludge, which contains 12 wt% potassium, the wastes do not contain significant amounts of potassium. The potassium passive-gamma signal gave an average of 17±2 pCi/g of K-40 between 2 and 5 ft below the surface. The K-40 signal was not analyzed quantitatively. It does show a general decrease in the waste zone and a return to approximately 20 pCi/g in the underburden. The K-40 signal was used to determine the location of three 745 sludge drums.[3]

5.6 Collateral Information

In the course of trying to determine the cause of the low moisture readings and evaluating the influence of chlorine, the importance of identifying the local media composition was recognized. An effort was made to identify specific waste forms using input from all four logging tools and comparing the set of results with expected waste signatures.

This effort resulted in the identification of twenty-three sets of signatures identifiable as waste forms. The number of each specific waste form identified corresponded reasonably well with the number expected based on the distribution of waste disposed of in the Stage I subsurface exploration area.

These results were originally prepared as part of this report, but were first published in detail as - Sections 5.6 and 5.7 in the OU 7-10 Stage I Subsurface Exploration and Treatability Studies Report,[3] and therefore are not reproduced in this report.

6. CONCLUSION

The classical neutron-based soil-moisture measurement technique, which relies on measuring thermal neutron flux, is inadequate by itself to determine moisture content in the waste zone. Soil with 22-vol% soil moisture contains approximately 1.8-wt% hydrogen. Two waste forms that account for most of the waste volume—Series 743 sludge and combustibles—have 4 to 6 times that much hydrogen from the oils, paper, and plastics within the wastes. Furthermore, the graphite wastes could be totally dry, and still result in thermal neutron flux orders of magnitude higher than expected from soil with 22-vol% moisture. Two other factors make correlating thermal neutron measurements to local moisture content difficult if not impossible—chlorine and heterogeneity of the waste zone.

Chlorine has a high neutron absorption cross section and therefore depresses the thermal neutron signal relative to that expected from thermalization of neutrons in a chlorine-free, hydrogen rich environment. The waste zone is highly heterogeneous. The neutron and neutron-gamma tools used have interrogation lengths of 6 to 18 in, and most of the time limited to less than a drum radius. This means that any particular measurement can be the result of an unknown combination of waste forms or voids, many of which have competing effects. However, the measurements will may represent a single waste form (when the probe casing has penetrated a drum), and more generally will be a combination of only the adjacent 2 or 3 drums and the nearby interstitial soil. It is less likely that 4, 5, or 6 drums contribute to a single measurement (but cannot exceed a very rare arrangement in which 14 drums could contribute).

Not only does the chlorine content contribute heavily to the under-representation of moisture (and hydrogen) concentration; it also causes an under-representation of itself. Understanding the chlorine concentration is important not only for interpretation of the neutron-based nuclear-logging data, but also in understanding the fate of chlorine in the SDA as a long-term performance assessment issue. It is recommended, therefore, that the n-gamma tool be calibrated for chlorine concentrations of 20 to 25 wt%.

Neutron logging measurements in the overburden and underburden indicate that these soils contain no major contaminants. Therefore, the neutron moisture measurements can be accepted as valid soil moisture measurements. The peak soil moisture content in the overburden and underburden was measured to be 20 – 26 vol%, similar to the soil moisture in nearby SDA calibration wells.

By the nature of moisture transport in soils, it is reasonable to conclude that the soil moisture, for the soil within the waste zone, is approximately 22-vol%. The moisture within any breached waste container, at a minimum, will be in equilibrium with the local soil, assumed to contain 22-vol% moisture. In the case of a breached nitrate waste, the final moisture content may be greater than 22-vol% due to the hygroscopic properties of the nitrate salts.

This page intentionally left blank.

7. REFERENCES

1. Arbon, R. E., *Nonmixed Waste Determination for IDC 300 Waste (Graphite Molds)*, INEEL/EXT-99-01137, 1999.

2. Baker, K., Internal Letter to James Okeson, *Pit 9 Moisture Content Measurements*, KEB-11-99, November 19, 1999.

3. BBWI, *OU 7-10 Stage I Subsurface Exploration and Treatability Studies Report (Draft)*, INEEL/EXT-2000-00403, July 2000.

4. Bechtel BWXT Idaho, LLC, *Preliminary Safety Assessment for the OU 7-10 Staged Interim Action Project Stage I, Phase II*, INEEL/EXT-98-00181, January 2000.

5. Bishop, C. W., *Soil Moisture Monitoring Results at the Radioactive Waste Management Complex of the Idaho National Engineering Laboratory, FY-96, FY-95, and FY-94*, INEEL/EXT-98-00941, 1998.

6. Bishop, C. W., Internal Letter CWB-009-99 to J. C. Okeson, *Estimate of Pit 9 Sediment Moisture Contents*, September 2, 1999.

7. Clawson, K. L., Start, G. E., and N. R Ricks, *Climatography of the Idaho National Engineering and Environmental Laboratory*, 2nd Edition, DOE/ID-12118, May 19, 1998.

8. Daniel B. Stephens & Associates, Inc., *Laboratory Analysis of Soil Hydraulic Properties of Radioactive Waste Management Complex Soil Samples*, May 1995.

9. Einerson, J. J., and R. W. Thomas, October 1999, *Pit 9 Estimated Inventory of Radiological and Nonradiological Constituents*, INEEL/EXT-99-00602.

10. External Letter, J. A. Van Vliet to G. L. Beausoliel, *Results of Moisture Logging From the Initial Probehole Installed in Pit 9, Operable Unit (OU) 7-10 Staged Interim Action Stage I, Phase I, At the Radioactive Waste Management Complex (RWMC)*, CCN# 00-002087, December 13, 1999.

11. Freeze, R. A. and J. A. Cherry, 1979, Groundwater, Prentice-Hall, Inc., Englewood Cliffs, NJ, 604 pp.

12. Glasstone, S. and A. Sesonske, Nuclear Reactor Engineering, Litton Educational Publishing, Inc., Van Nostrand Reinhold Company, New York, NY, 1967.

13. Jury, W. A., Gardner, W. R., and W. H. Gardner, Soil Physics, 5th Edition, John Wiley and Sons, Inc., New York, NY, 1991.

14. LANL, *Passive Nondestructive Assay of Nuclear Materials*, NUREG/CR-5550, LA-UR-90-732, March 1991.

15. Lee, J-H., G. P. Martins, and J. R. Weidner, *Characterization Studies on: (A) Contaminated Batch of Rocky Flats Soil, (B) Uncontaminated Batch of INEL Soil*, EGG-WTD-974, June 01, 1991.

16. Loomis, G. G., A. P. Zdinak, and C. W. Bishop, *Innovative Subsurface Stabilization Project – Final Report*, INEL-96/0439, November 1996.

17. Low, J. O., *Annual Technology Assessment - Progress Report TRU Buried Waste Program (BWP) INEL*, EGG-2429, December 1985.

18. McElroy, D. L., *Soil Moisture Monitoring Results at the Radioactive Waste Management Complex of the Idaho National Engineering Laboratory*, EGG-WM-11066, 1993.

19. Martin, K. L., et al., *Preliminary Assessment of Surface Soils at Active EG&G Idaho Facilities Data Document*, EGG-ESQ-9225, September 1990.

20. Perry, R. H., D. W. Green, and J. O. Maloney, Editors. Chemical Engineers Handbook, Sixth Edition, McGraw-Hill, New York, NY, 1984.

21. Porro, Indrek and K. N. Keck, *Summary of Activities at the Engineered Barriers Test Facility, October 1, 1995, to January 31, 1997, and Initial Data*, INEEL/EXT-97-00239, March, 1997.

22. Schuman, R. P. and R. L. Tallman, *Properties of Rocky Flats Waste Sludges*, RE-M-81-011, November 1981.

23. Shaw, P. G., B. Anderson, and D. E. Davis, *Laboratory Scale Vitrification of Low Level Radioactive Nitrate Salts & Soils from INEL*, EGG-WTD-10640, July 1, 1993.

24. U. S. Department of Energy, Idaho Operations Office, *Annual Progress Report: FY-1986*, DOE/ID 10153, 1986.

25. WMTS, Waste Management Technical Services, *Interim Report of Geophysical Logging at Pit 9, INEEL*, Draft, Unnumbered, April 17, 2000.